Two fixed beam slotted stripline antenna arrays

Breithaupt, R. W.; Clarke, B.

https://doi.org/10.4224/21276074

Report (National Research Council of Canada. Radio and Electrical Engineering Division : ERB), 1969-04

ERB - 826

UNCLASSIFIED

NATIONAL RESEARCH COUNCIL OF CANADA

RADIO AND ELECTRICAL ENGINEERING DIVISION

TWO FIXED BEAM SLOTTED STRIPLINE ANTENNA ARRAYS

BY

- R. W. BREITHAUPT AND B. CLARKE -

OTTAWA

APRIL 1969

ABSTRACT

The design, construction, and performance of two stripline antenna arrays to be used as fixed beam altimeter antennas is described. These traveling wave arrays contain 8 X 10 and 16 X 21 series slots, respectively, and employ combination series–parallel feeds. The parallel feed junctions are folded onto the rear of the antenna using resonant slot coupling. Each row of series slots is terminated by a series flat load involving no ground plane connection.

Design data to give the required resonant slot resistances were computed from an expression which includes the effect of internal, but not external coupling, and transmission line attenuation between slots.

CONTENTS

FIGURES

TABLES

TWO FIXED BEAM SLOTTED STRIPLINE ANTENNA ARRAYS

– R.W. Breithaupt and B. Clarke –

1. Introduction

Two fixed-beam antennas were developed as part of a radar altimeter for forest inventory [1, 2, 3] requested by the Department of Forestry and Rural Development. Separate antenna configurations were requested for two surveying altitude ranges – less than 1000 feet and 1000–2000 feet. Two antennas, to transmit and receive, having beamwidths of $\cong 12°$ were required for the lower altitude range; and a single antenna having a 3-db beamwidth of $\cong 5°$ was required for the higher altitude range. A thin planar antenna structure was specified both for aerodynamic reasons and for ease of mounting on light aircraft. Furthermore, it was considered necessary to have essentially the entire face of the aperture radiating, with a minimum of this area associated with the feed structure.

A summary of the specifications requested for the two antennas is given in the following table.

TABLE I

Characteristics requested for two altimeter antennas

Center frequency	4.2 GHz	Same
Bandwidth	5%	Same
Beamwidth (3 db)	12°	5°
Average power	2 W	Same
Peak power	2 kW	Same
Sidelobes	-15 db	-12 db
Input VSWR	<1.6	Same

A slotted stripline antenna configuration was used as it appeared to best provide these characteristics. Such a two-dimensional array contains series-fed traveling wave arrays in the E plane, parallel-connected at the feed end to provide a suitable H-plane pattern. The parallel connections are folded onto the rear of the radiating portion of the antenna so that radiating slots fill the entire aperture uniformly.

Although a large body of knowledge concerning general two-dimensional arrays is available, little has been published on the design aspects of a two-dimensional stripline array employing series slots. A review of early stripline antenna work may be found in the Triplate Handbook [4] or in Microwave Engineering [5]. More recent work, such as that by Jones [6] or Johnson [7] is also noteworthy.

A partial description of results for the smaller antenna can be found in the NRC REED Bulletin [8].

The following section contains a design analysis of a traveling wave array, and, after a section on component design data, the small 8 X 10 slot and larger 16 X 21 slot arrays are dealt with individually.

2. Traveling Wave Array Analysis for Series Elements

Analysis of a series-fed traveling wave antenna employing series radiating elements has been given elsewhere, [9] but will be included here for completeness and also so that the associated computer program may be easily understood. The effects of transmission line loss, multiple internal transmission line reflections, and variable spacing are usually included in this analysis to produce radiating element resistances (whose associated reactances are known). If the reactance of a radiating element cannot be varied for a given resistance, and if multiple reflections between elements are considered, then the interelement spacing must be varied in order to maintain phase as well as amplitude control over the resulting aperture distribution.

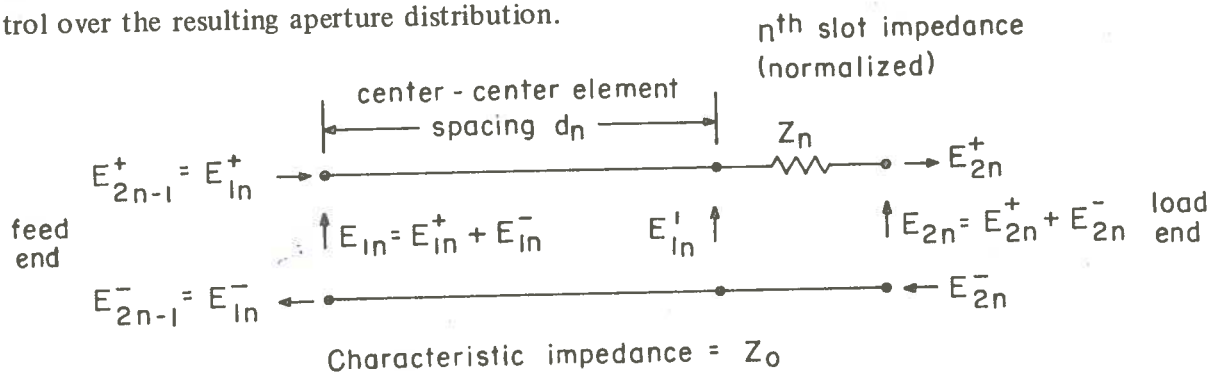

Figure 1 Equivalent circuit for radiating element and transmission line section

Consider an N element, series-fed array where d_n is the spacing between the $(n-1)^{th}$ and n^{th} elements. A transfer matrix can be written for a section containing the n^{th} radiating element and transmission line section d_n, as shown in Fig. 1. The +, - superscripts indicate traveling waves toward the load and feed ends, respectively. The transfer matrix relating input and output voltages for this equivalent circuit is

$$\begin{pmatrix} E^+_{1n} \\ E^-_{1n} \end{pmatrix} = \begin{pmatrix} \exp(\alpha + i\beta)\, d_n & 0 \\ 0 & \exp -(\alpha + i\beta)\, d_n \end{pmatrix} \begin{pmatrix} 1 + Z_n/2 & -Z_n/2 \\ Z_n/2 & 1 - Z_n/2 \end{pmatrix} \begin{pmatrix} E^+_{2n} \\ E^-_{2n} \end{pmatrix} \quad (1)$$

where α, β are the effective attenuation and propagation constants of the transmission line. It can easily be shown that the real power P_{rn} radiated by the n^{th} element is

$$P_{rn} = \frac{|E'_{1n} - E_{2n}|^2}{\mathrm{Re}(Z_n)\, Z_0} \quad (2a)$$

or

$$P_{rn} = \frac{|E_{1n}^{+\prime}|^2}{Z_0} + \frac{|E_{2n}^{-}|^2}{Z_0} - \frac{|E_{1n}^{-\prime}|^2}{Z_0} - \frac{|E_{2n}^{+}|^2}{Z_0} \tag{2b}$$

$$= \frac{\mathrm{Re}(Z_n)}{Z_0} |E_{2n}^{+} - E_{2n}^{-}|^2 \tag{2c}$$

$$= \frac{\mathrm{Re}(Z_n)}{Z_0} |E_{1n}^{+\prime} - E_{1n}^{-\prime}|^2 \tag{2d}$$

The element resistance $\mathrm{Re}(Z_n)$ may be obtained from equation 2c where

$$\mathrm{Re}(Z_n) = \frac{P_{rn} Z_0}{|E_{2n}^{+} - E_{2n}^{-}|^2} \tag{3}$$

If P_{tn} is the net real power transmitted toward the load at the E_{2n} terminals,

$$P_{tn} = \frac{|E_{2n}^{+}|^2}{Z_0} - \frac{|E_{2n}^{-}|^2}{Z_0} \tag{4}$$

Substitute for Z_0 in equation 3 from equation 4 to write $\mathrm{Re}(Z_n)$ in another form, namely

$$\mathrm{Re}(Z_n) = \left[\frac{P_{rn}}{P_{tn}}\right] \left[\frac{|E_{2n}^{+}|^2 - |E_{2n}^{-}|^2}{|E_{2n}^{+} - E_{2n}^{-}|^2}\right] \tag{5a}$$

$$= \left[\frac{P_{rn}}{\sum_{s=n+1}^{N} P_{rs} + P_{Ln}}\right] \left[\frac{|E_{2n}^{+}|^2 - |E_{2n}^{-}|^2}{|E_{2n}^{+} - E_{2n}^{-}|^2}\right] \tag{5b}$$

where P_{Ln} is the total real power supplied to transmission line losses from $s = n+1 \rightarrow N$ and to the load. It is expressed

$$P_{Ln} = \sum_{s=n+1}^{N} \left[\frac{|E_{1s}^{+}|^2}{Z_0} [1 - \exp(-2\alpha d_s)] - \frac{|E_{1s}^{-}|^2}{Z_0} [1 - \exp(+2\alpha d_s)]\right] + P_{\mathrm{load}} \tag{6}$$

The form given by equation 5b is interesting because the first quantity is that which would be obtained assuming no multiple reflections (i.e., $E_{1n}^{-} = E_{2n}^{-} = 0$) between elements on the transmission line.

The electric field strength E_n in the resulting aperture distribution is

$$E_n = C_1 \left(\mathrm{Re}(Z_n)\right)^{1/2} (E_{2n}^{+} - E_{2n}^{-}) \tag{7}$$

where C_1 is a constant.

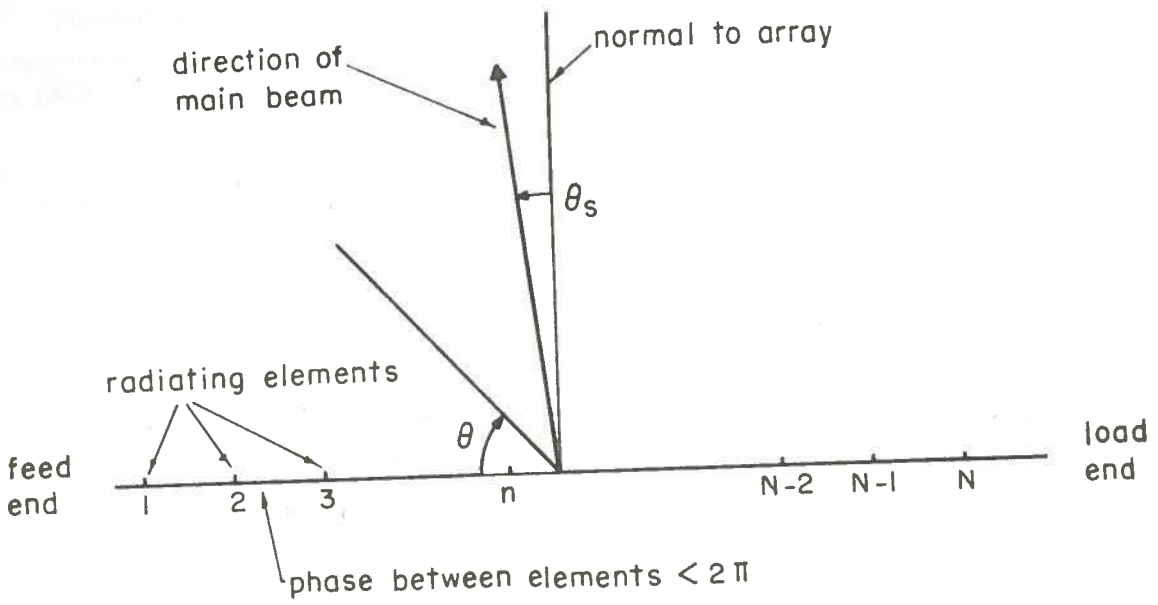

Figure 2 Definition of squint angle

If a squint angle θ_s is desired (see Fig. 2), then the spacing d_n required for the appropriate plain phase front is determined by solving

$$d_n = [\arg(E_n) - \arg(E_{n-1})] \frac{\lambda_0}{2\pi \sin\theta_s} \tag{8}$$

where equations 7 and 1 are used to write $\arg(E_{n-1})$ in terms of d_n, and λ_0 is the free space wavelength. This gives

$$d_n = \left[\arg(E^+_{2n} - E^-_{2n}) - \arg\left\{\left[(1 + Z_n/2)\,E^+_{2n} - (Z_n/2)\,E^-_{2n}\right]\exp(\alpha + i\beta)d_n - \left[(Z_n/2)E^+_{2n} + (1 - Z_n/2)E^-_{2n}\right]\exp -(\alpha + i\beta)d_n\right\}\right] \frac{\lambda_0}{2\pi \sin\theta_s} \tag{9}$$

If a constant spacing d is desired (for resonant elements, say, where a small aperture phase error can be tolerated), then equation 9 reduces to

$$d = \frac{\lambda_0}{\frac{\lambda_0 \beta}{2\pi} + \sin\theta_s} \tag{10}$$

The stripline antennas to be described employed equation 10 above, with nearly resonant slots.

It is necessary to specify power to the load P_{load}, power radiated by each element, propagation and attenuation constants, and the function $\mathrm{Im}(Z_n)$ versus $\mathrm{Re}(Z_n)$, in order to find

element resistances $\mathrm{Re}(Z_n)$ and spacings d_n which produce a desired aperture distribution (both amplitude and phase). Beginning with $n = N$, equations 3 and 9 or 10 are used to find $\mathrm{Re}(Z_N)$ and d_N. Then, by repeating the process, using equation 1, successively for $n = N-1, \ldots\ldots 1$, one obtains all values of $\mathrm{Re}(Z_n)$ and d_n. The VSWR looking into the transmission line at the n^{th} element, is

$$\mathrm{VSWR}_n = \frac{|E_{1n}^+| + |E_{1n}^-|}{|E_{1n}^+| - |E_{1n}^-|} \tag{11}$$

The electric field radiation pattern in the plane of the array is obtained from

$$E(\theta) = f(\theta) \sum_{n=1}^{N} E_n \exp - i\left(n - \frac{N+1}{2}\right) \frac{2\pi d_n}{\lambda_0} \cos\theta, \tag{12}$$

where $f(\theta)$ is the element pattern and θ is defined in Fig. 2.

Appendix A contains a program written in Fortran IV which, for uniform spacing, resonant elements, and an input as specified below, produces an output as indicated.

Input

Desired aperture distribution $|E_{rn}|$
Power to the load P_{load}
Slot spacing d
Effective wavelength $2\pi/\beta$ in waveguide
Frequency f in GHz
Effective waveguide attenuation α
A set of slot resistances and reactances (optional)

Output

Element resistance $\mathrm{Re}(Z_n)$ to give desired aperture distribution, with resulting amplitude and phase of aperture distribution

VSWR for above

Amplitude and phase of aperture distribution resulting from the set of slot resistances in the input above, plus a printed and plotted E-plane radiation pattern for this.

3. Experimental Data and Component Design

The Impedance of Offset Series Slots in Stripline

The variation of impedance of a radiating element with variations of appropriate physical parameters must be determined either analytically or experimentally, in order to design for a desired aperture distribution. An offset series slot in stripline, which is used for these altimeter antennas, and a simple equivalent circuit are shown in Fig. 3.

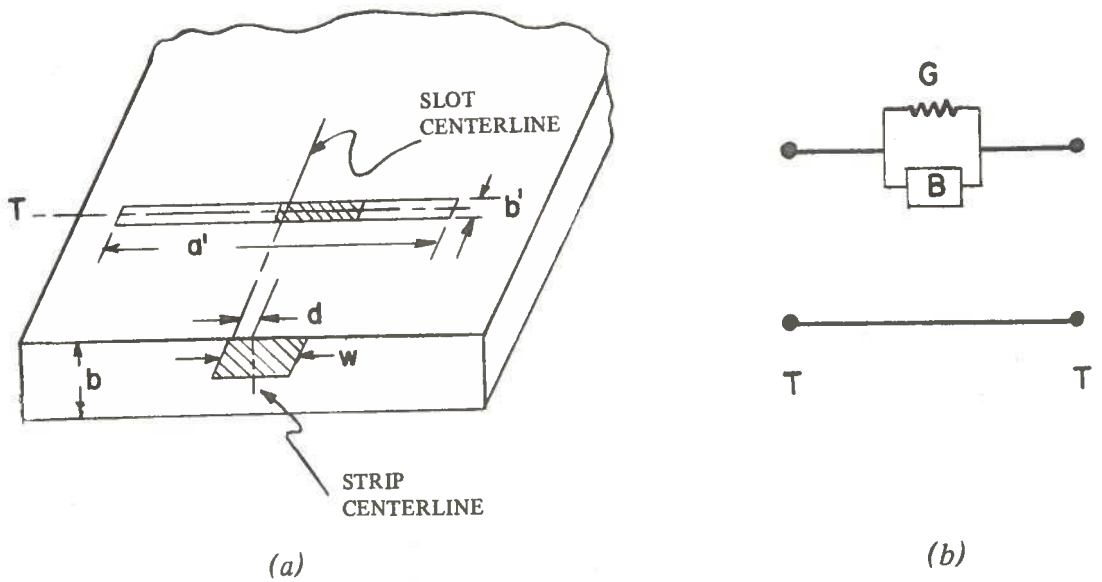

Figure 3 (a) Offset series slot configuration, (b) Equivalent circuit

An analytical investigation of the variation of slot conductance G with offset d was made for various values of ground plane spacing b and has been presented elsewhere [10], so will not be repeated here.

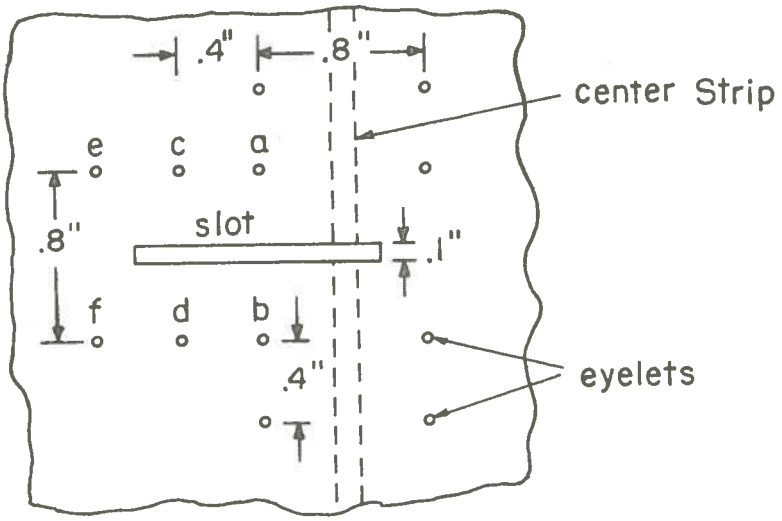

Figure 4 Eyelet configuration to suppress spurious modes

Experimental slotted line measurements were also made at $f = 4.2$ GHz. To suppress spurious stripline and parallel plate modes, eyelets ($\frac{3}{32}$-inch diameter) were placed around the slot and center strip as shown in Fig. 4, to maintain the ground planes at the same potential [11].

An effective short circuit of the transmission line was obtained at the slot center line by terminating the center strip in an open circuit $\cong \frac{3}{4}\lambda_g$ beyond the center line (allowing for fringing capacitance of the open circuit [12]). A Weinschel coaxial slotted line was used, with the coax–stripline adapter matched by a five-screw stripline tuner (resulting VSWR < 1.02). Stripline transmission loss was corrected for in these slot impedance measurements. A long transverse strip 0.1 inch wide was etched on one ground plane, eyelets were inserted as shown in Fig. 4, and slot offset and length were varied by applying and removing silver conductive paint on the etched strip. Rexolite 1422 copper clad laminate was used, with ground plane spacing $b = 0.250$ inch, and a characteristic impedance of 50 ohms for stripwidth $w = 0.182$ inch ($\epsilon_r = 2.53$). The lower limit of measurable slot impedance was determined essentially by the residual transmission line VSWR of $\cong 1.02$. Slot impedances obtained are presented graphically on the Smith chart in Fig. 5.

Some tests were made to determine differences between active slot impedance in an infinite E- or H-plane array and the impedance of an isolated element, by placing reflectors at suitable spacings on either side of the slot in the E or H plane. As expected, reflectors placed parallel to the E plane indicated virtually no H-plane coupling between radiating elements. Reflectors placed parallel to the H plane indicated a moderate change of slot impedance for E-plane coupling between slots. A point is plotted on the Smith chart of Fig. 5 giving the active impedance of a slot ($a' = 1.8$ inches, $d = 0.55$ inch, $b' = 0.10$ inch, $b = 0.250$ inch) with reflectors simulating 1.531 inches E-plane slot spacing.

Tests were also made to observe the effect of removing various eyelets as shown in Fig. 4. For a slot ($a' = 1.25$ inch, $d = 0.55$ inch, $b' = 0.100$ inch, $b = 0.250$ inch) measured at 4.2 GHz the results were as follows.

	VSWR	minimum position (mm)
All eyelets in	3.95	92.7
e, f out	4.6	92.4
c, d out	9.5	92.2
a, b out	12.5	92.7

In view of the large impedance changes with and without certain eyelets, it is interesting to note that the theoretical resonant resistance (based on a model with no eyelets) gave very similar results to those for the experimental model used in Fig. 4 [10], indicating that the presence of eyelets simply changes the slot reactance.

Resonant Slot Coupler

Two methods of connecting the radiating portion of the antenna to the feed section were investigated. One method employed a simple U bend of the entire stripline and will be described subsequently. In the other method, a resonant slot coupled energy from one board to the other, as shown in Fig. 6.

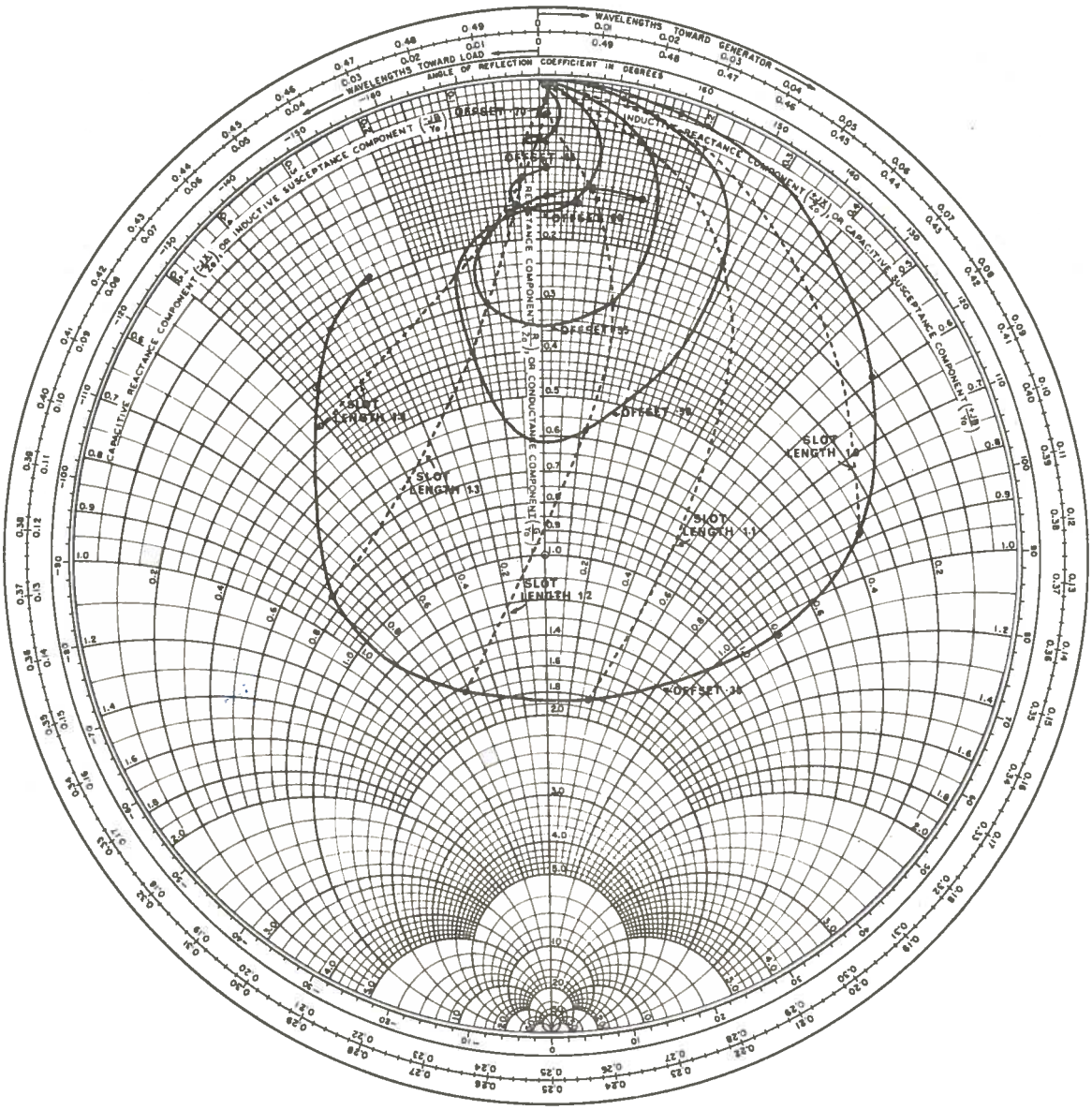

Figure 5 Measured impedance of an offset series slot in stripline

f = 4.2 GHz	ϵ_r = 2.53
Z_0 = 50 ohms	b' = .100 inch
b = .250 inch	a' = slot length
w = .182 inch	d = offset

Rexolite 1422 laminate

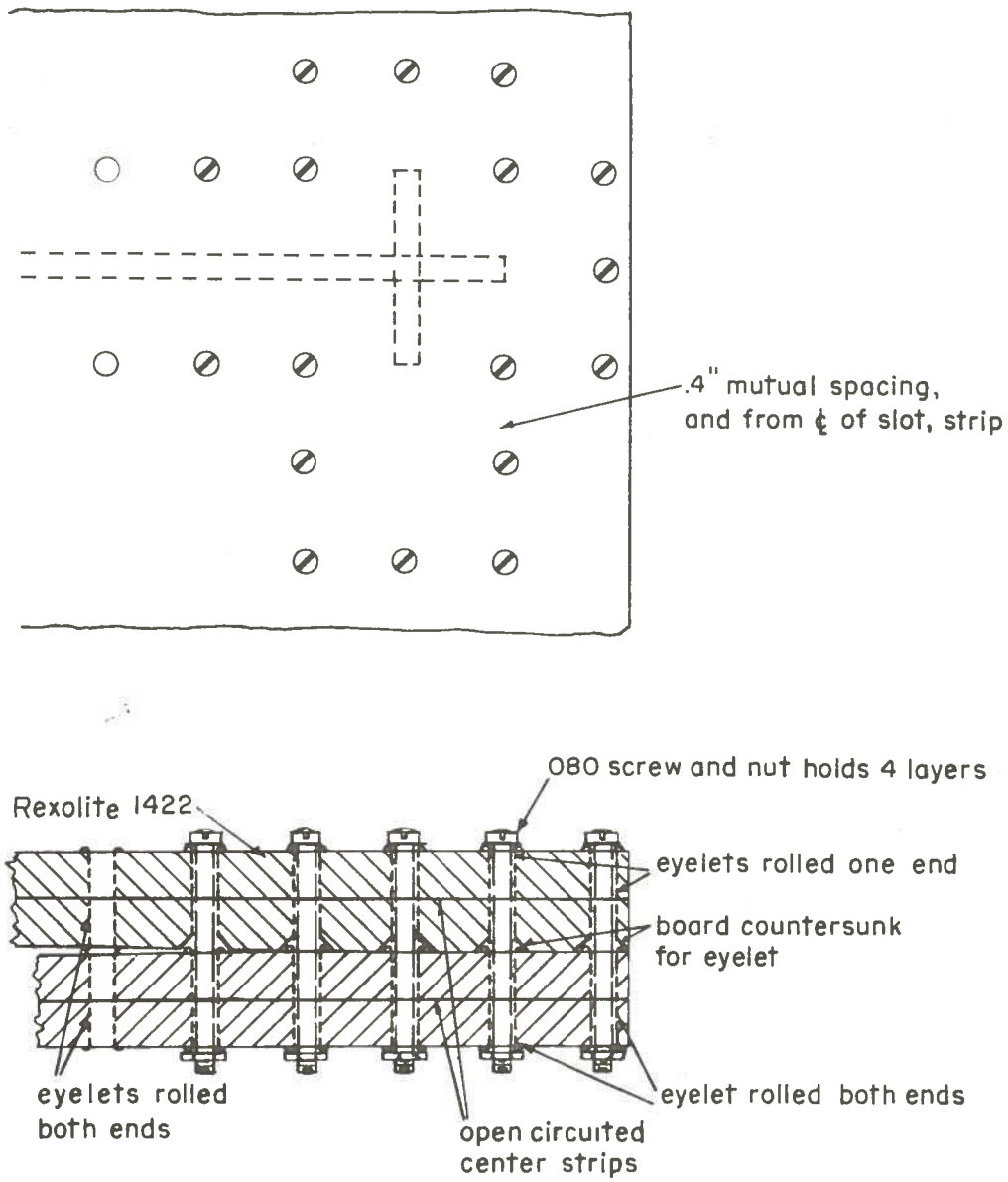

Figure 6 Resonant slot coupler

Open circuited center conductors are used so that either transmission line sees the loaded slot impedance, which was adjusted to 50 ohms (resonant) by proper selection of offset and length. Eyelets were employed with 0.4-inch mutual spacing as before, to eliminate spurious modes which would provide leakage and coupling to other transmission lines.

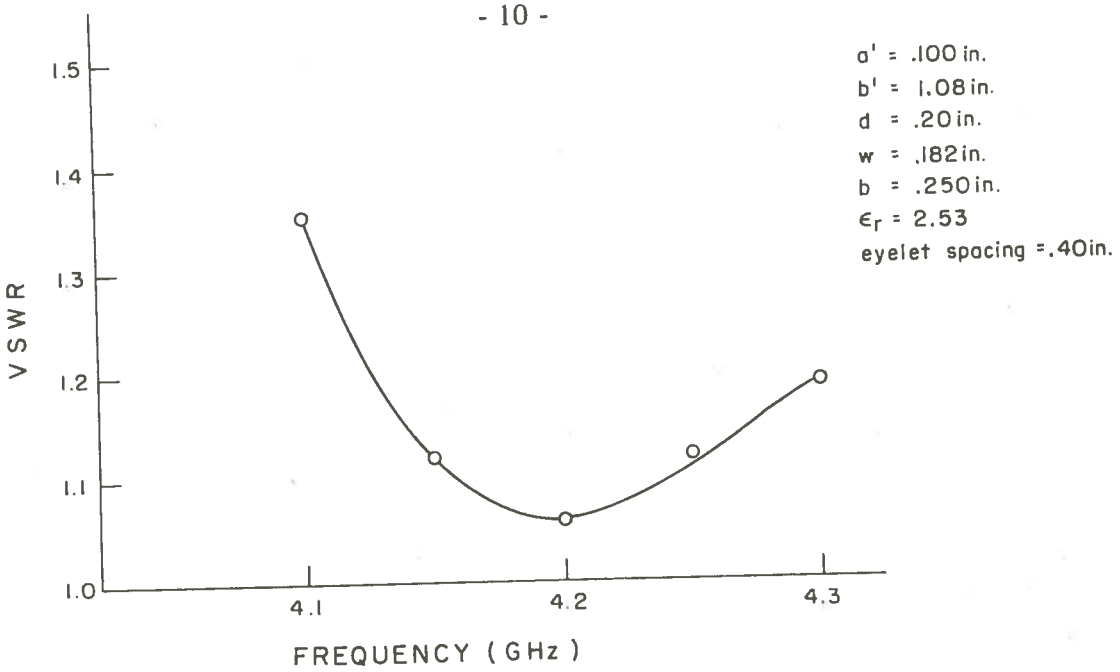

Figure 7 VSWR of resonant slot coupler

A plot of the VSWR–frequency characteristic obtained is given in Fig. 7. It is clear that the advantage gained in convenience of assembly of the radiating and feed portions is offset by the relatively narrow bandwidth due to the resonant slot.

U Bend

This broadband bend is shown in Fig. 8, and provides a VSWR < 1.2 over a wide frequency band. The outer ground plane of the bend is copper foil soldered along the seams on either end of the U. A strip of 0.015-inch thick shim stock provides a small radius of curvature for the inner ground plane. The chief disadvantage of this bend is difficulty in assembly.

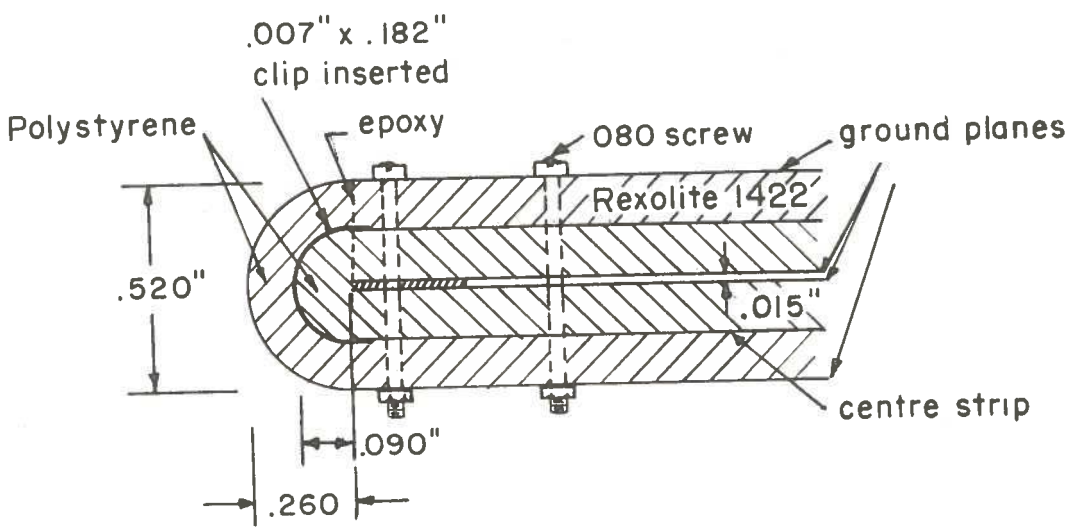

Figure 8 U bend, side view

Flat Loads

Several types of flat load were employed. A tapered strip of synthane $\frac{1}{32}$-inch or $\frac{1}{16}$-inch thick and several wavelengths long, was used flat on the center strip to absorb power gradually, and was convenient for a moving load. Another version of this had the center strip etched in a spiral containing $\cong 2$ wavelengths, and either a fixed or rotating piece of synthane was used for a fixed or variable length load. The VSWR of the above loads was $\cong 1.10$.

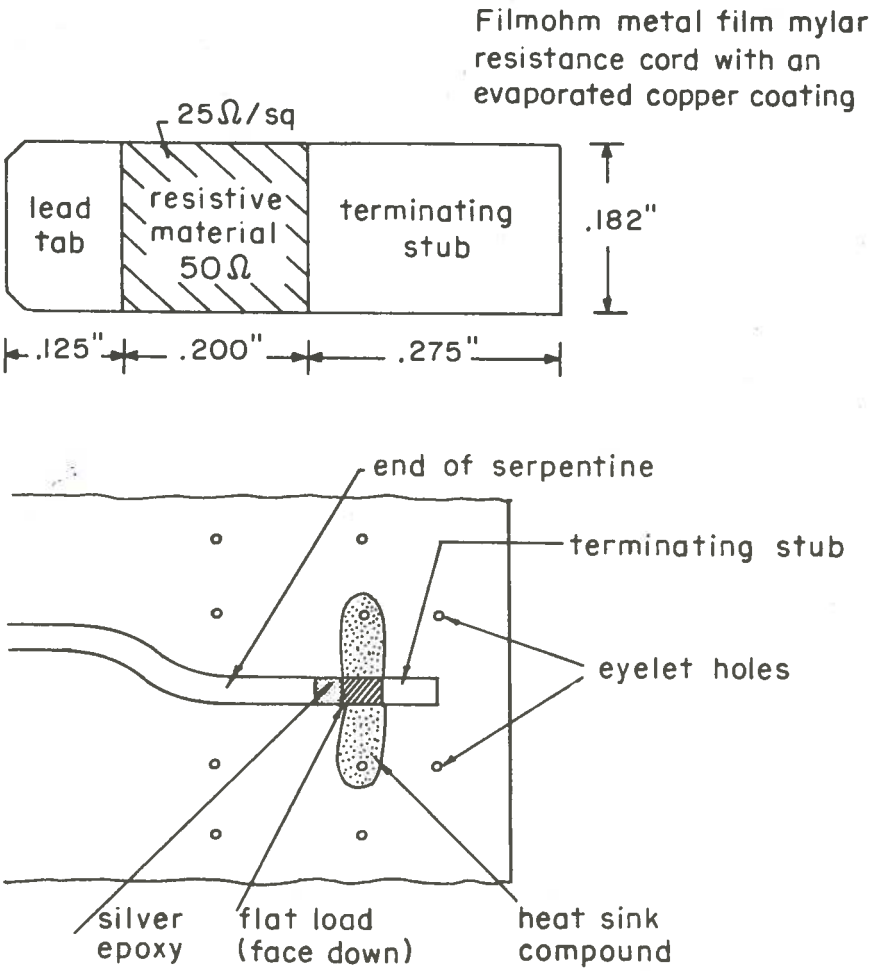

Figure 9 Stripline termination

A much better (although narrower band) method consists of a 50 ohm resistance in series with the center strip, followed by an effective quarter wavelength of open circuited center strip. The length was determined experimentally because the resistance does not act entirely as a lumped element at a known point on the transmission line. A suitable resistive element can be made by evaporating or painting a conductive coating on a mylar based resistive material which is commercially available (Filmohm metal film mylar resistance card). The ohms/square or area of resistance material used is a compromise between bandwidth and power handling capacity. A description of the termination used is given in Fig. 9. Good conductive contact between the lead tab and center strip is ensured by a silver epoxy bond. A wideband commercial

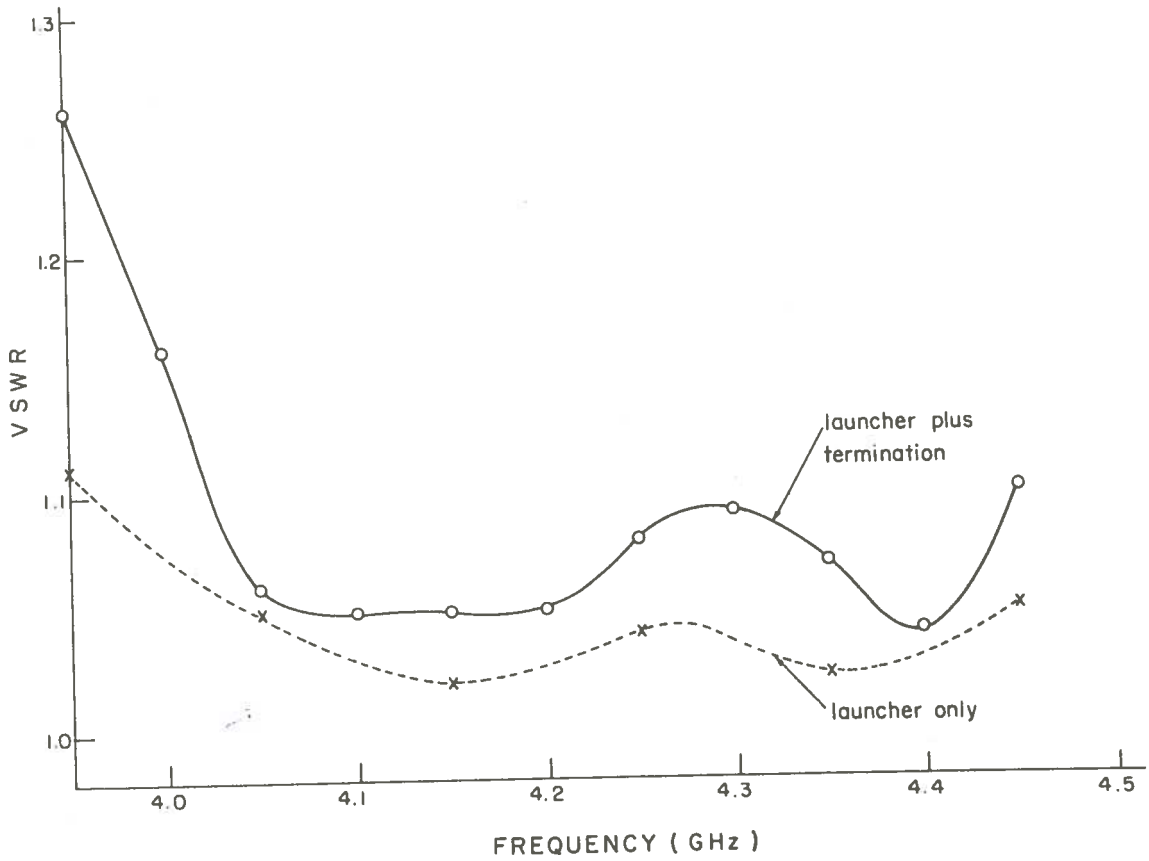

Figure 10 Frequency response of stripline termination

'pill' termination (E.M.C. Technology) also provides a series 50 ohm load which is attached to one of the ground planes, thus providing a higher power capability. However, for a modest bandwidth requirement (<10%), the type of termination described in Fig. 9 is more convenient to install. Heat sink compound can be applied as shown in Fig. 9, to raise the power capacity to 100 mW. The VSWR–frequency characteristic is plotted in Fig. 10. Characteristics of commonly used terminations may also be found in section 4 of reference 4 although this work is out of date.

Phase Shifter

The type of phase shifter used is described, page 61 of reference 10, and is adjusted by means of a recessed screw as shown in Fig. 11. The upper and lower halves of the stripline board were held apart slightly for phase adjustment by screws temporarily

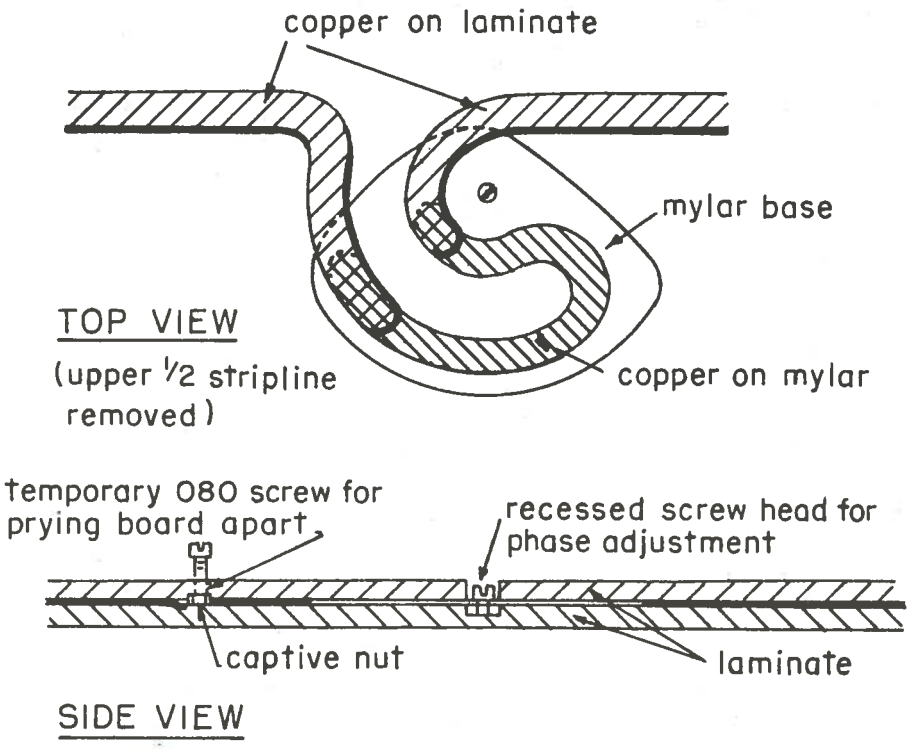

Figure 11 360° phase shifter

inserted in captive nuts in the board (see Fig. 11). A large number of eyelets was necessary for spurious mode suppression. Fine phase adjustment was difficult to achieve due to variable contact resistance and a generally poor mechanical arrangement, so that the use of adjustable phase shifters in these antennas was eliminated.

Assembly Precautions

Artwork was done three times full scale with a resulting full scale error of $\cong \pm 0.002$ inch. It was important to maintain a close tolerance on slot offset as r_n is very sensitive to changes in offset for small r_n [10]. There was considerable leakage of energy from the edge of the boards in the parallel feed section before eyelets were added throughout with 0.4 inch mutual spacing for spurious mode suppression. The edge of the board, as well as all openings at eyelets, etc., were sealed to prevent moisture from entering between dielectric slabs. Large slot impedance changes, and an unbalanced transmission line resulted from moisture adjacent to the eyelets and center strip.

Eyelets were carefully seated and rolled, as any extra spacing between dielectric slabs and/or any lack of good electrical contact with both ground planes also caused large changes in slot impedance and unbalance of the transmission line configuration.

Some experiments were made with electroless copper plating of the dielectric in order to plate through eyelet holes and avoid using eyelets. The electroless copper plating

did not satisfactorily cross the junction between dielectric slabs halfway along the hole, however, and this technique was not used.

4. 8 X 10 Slot Arrays

The general specifications chosen for this array are given in Table II:

TABLE II

General specifications for 8 X 10 slot array

f_0	4.2 GHz
Δf	5%
3 db beamwidth	$<12°$
$P_{avg.}$	3 W
P_{peak}	5 kW
P_{load}	$\sim 20\%$
θ_s	$\sim 5\%$
aperture distribution	Tschebyscheff -25 db S/L
sidelobes desired	-18 db
slots/row	10
no. rows	8
d	1.531 inch (constant)
row spacing	2.060 inch
aperture size	17 X 17 inch
ϵ_r	2.53 (rexolite 1422)
k(nominal)	$1.10 = \frac{\text{serpentine length between slots}}{d}$
b	0.250 inch

One-Dimensional 10-Slot Array

Three different one dimensional series fed test arrays were constructed, but only the model shown in Fig. 12 which incorporates the final design parameters will be described here. A Tschebyscheff theoretical aperture distribution was obtained from tables [13] for -25 db sidelobes, and values of $\mathrm{Re}(Z_n)$ were calculated for the ten slots assuming multiple internal reflections, resonant elements, and using the analysis of section 2 for constant spacing. Due to a small error in the original program a slightly incorrect set of slot resistances was calculated and used. Zero transmission attenuation was assumed for

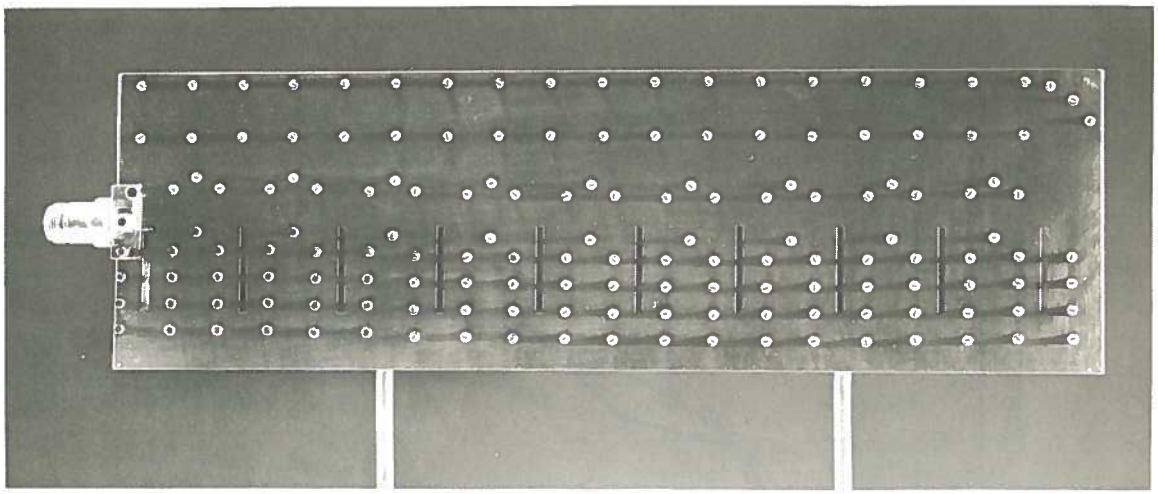

Figure 12 One dimensional 10 slot array

this calculation. These slot resistances, together with appropriate slot offsets and lengths which were taken from Fig. 5 and reference 10, are given in Table III.

TABLE III

Slot parameters used for 10-slot one-dimensional array

Slot No.	Tschebyscheff −25 db S/L aperture distribution (fld.)	Slot resistance used $\mathrm{Re}(Z_n)$	Slot length used a' (inches)	Slot off-set used d (inches)
1	1.995	0.0197	1.18	0.700
2	2.553	0.0321	1.27	0.700
3	3.643	0.0677	1.265	0.656
4	4.542	0.1189	1.265	0.616
5	5.050	0.1904	1.27	0.590
6	5.050	0.2928	1.27	0.564
7	4.542	0.3983	1.27	0.538
8	3.643	0.3479	1.27	0.550
9	2.553	0.1842	1.27	0.591
10	1.995	0.1141	1.265	0.619

The resulting measured aperture distribution and E-plane radiation pattern for this one-dimensional array are not given here, as they are nearly identical with those obtained for the two-dimensional 8 X 10 slot array, which are given in Figs. 13 and 14 respectively, for $f = 4.2$ GHz.

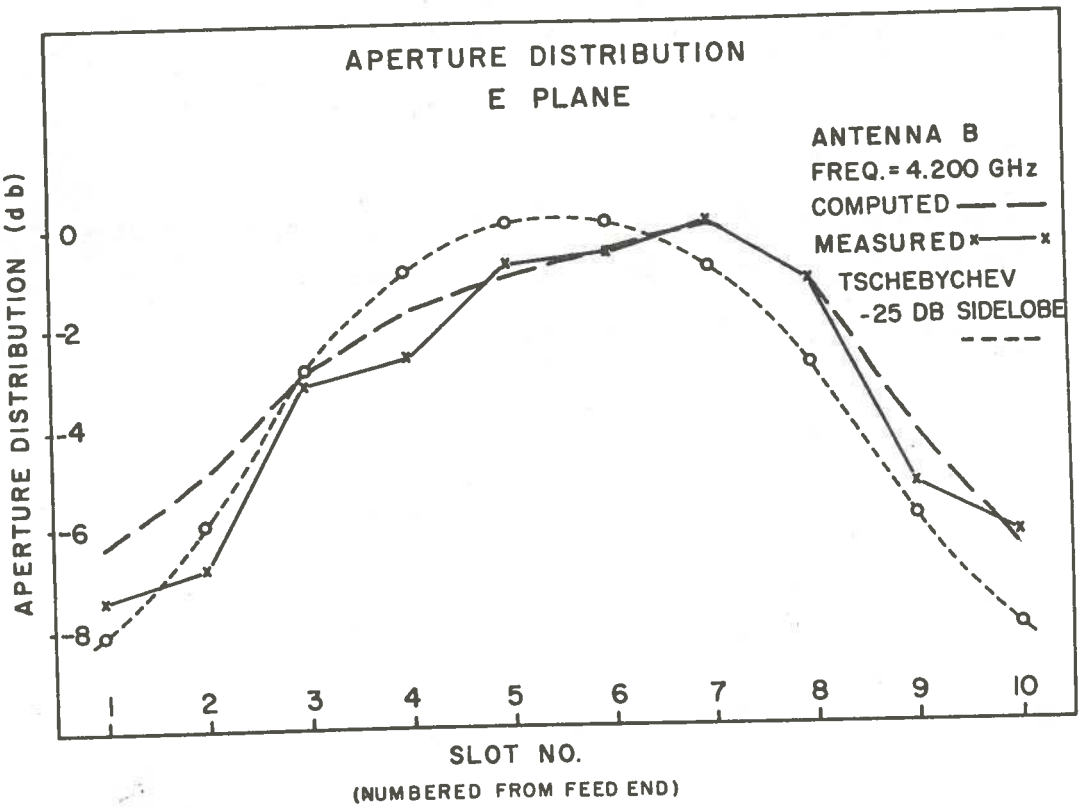

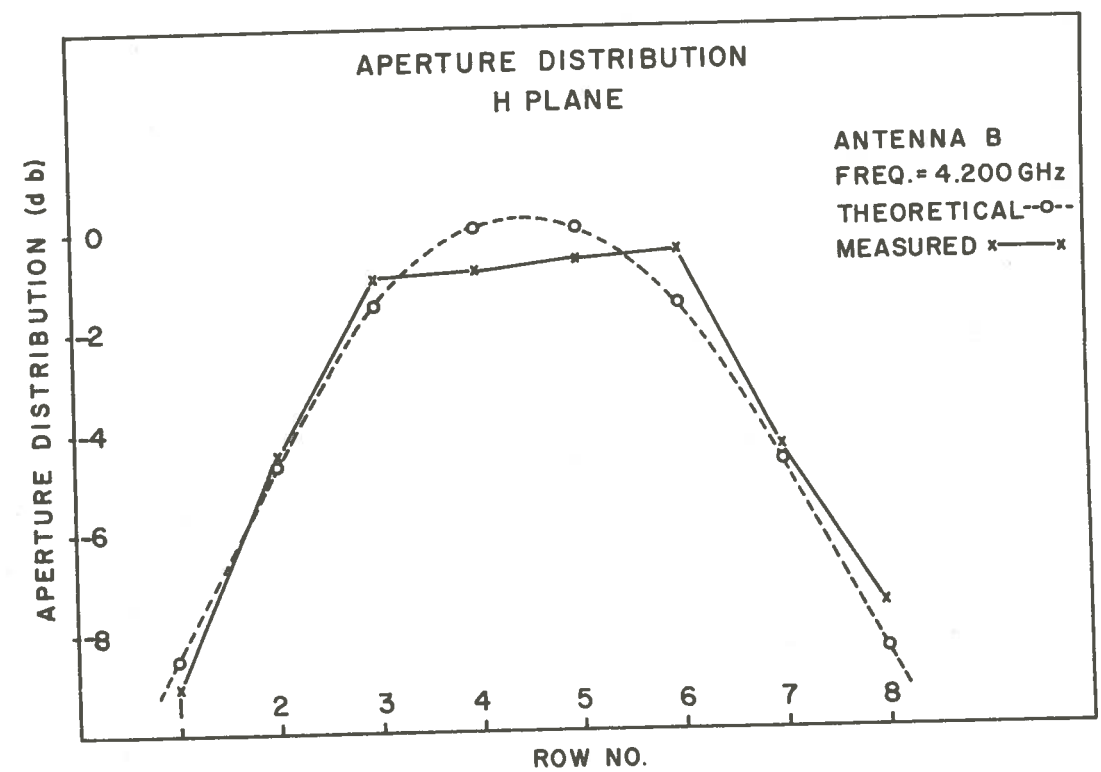

Figure 13 Aperture distribution of the 8 X 10 slot array

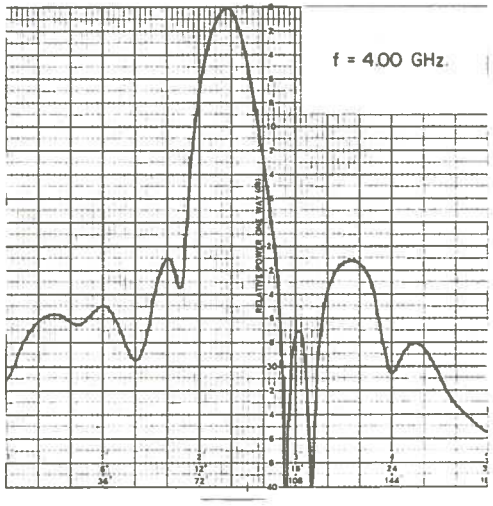

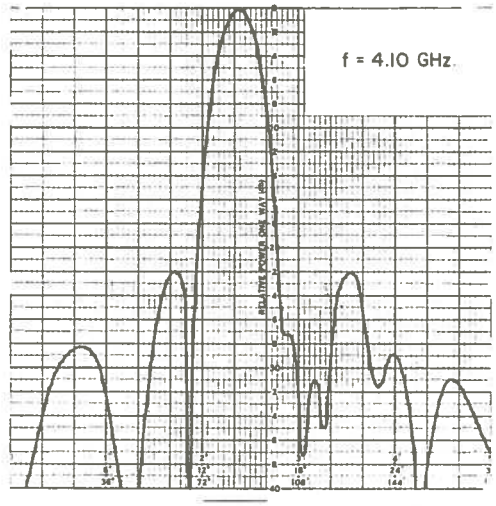

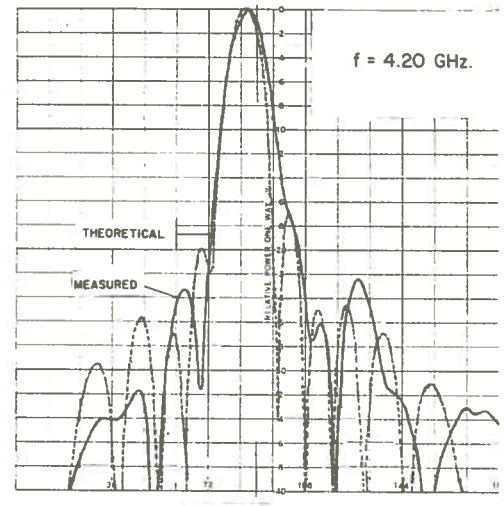

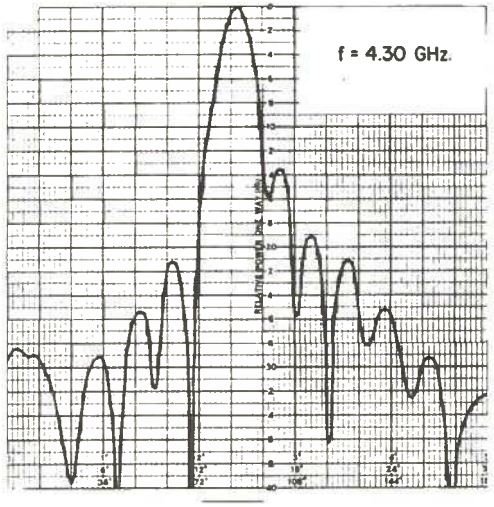

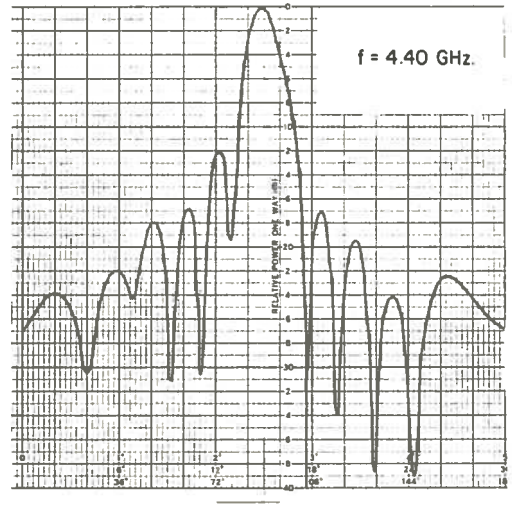

Figure 14 (a) Radiation patterns of the 8 X 10 slot array, E plane

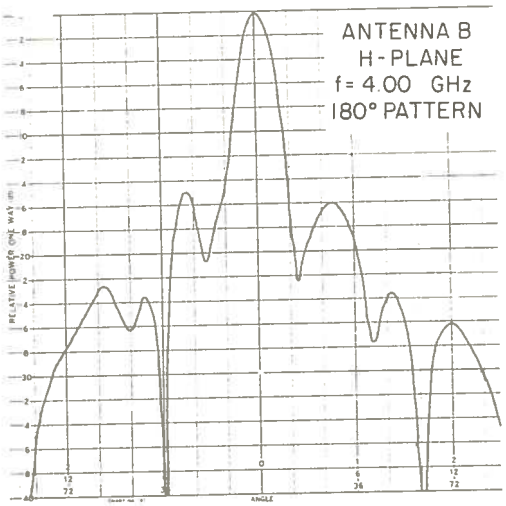

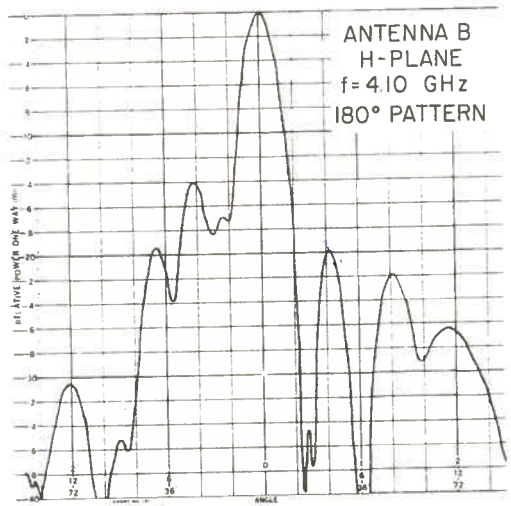

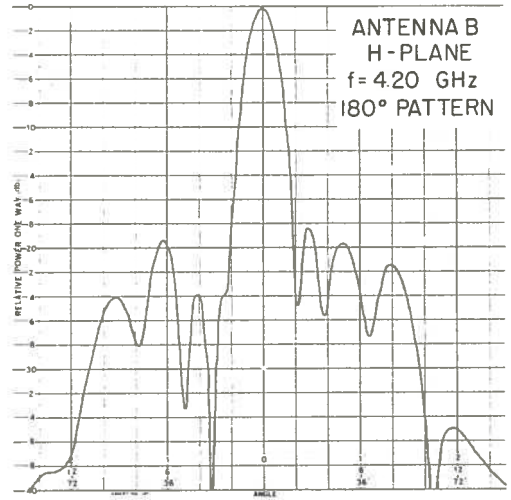

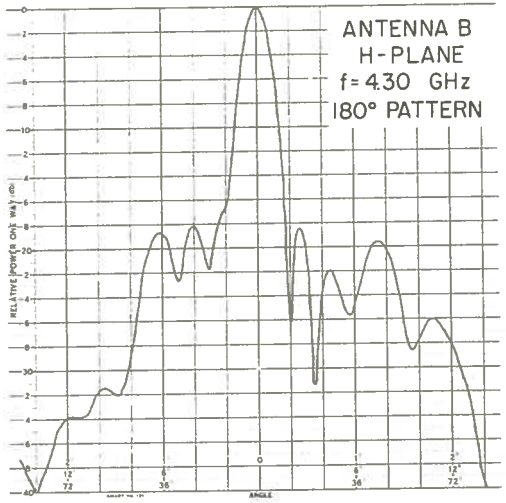

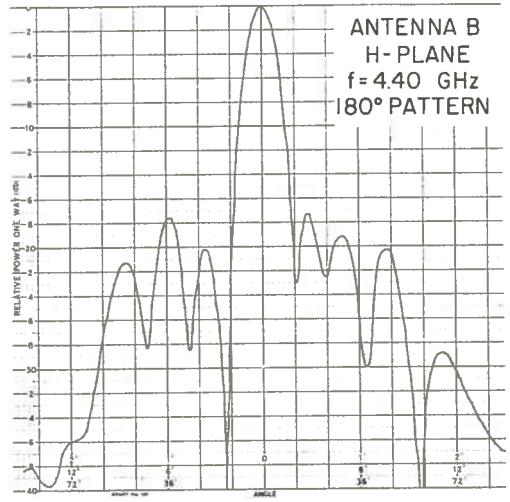

Figure 14 (b) Radiation patterns of the 8 X 10 slot array, H plane

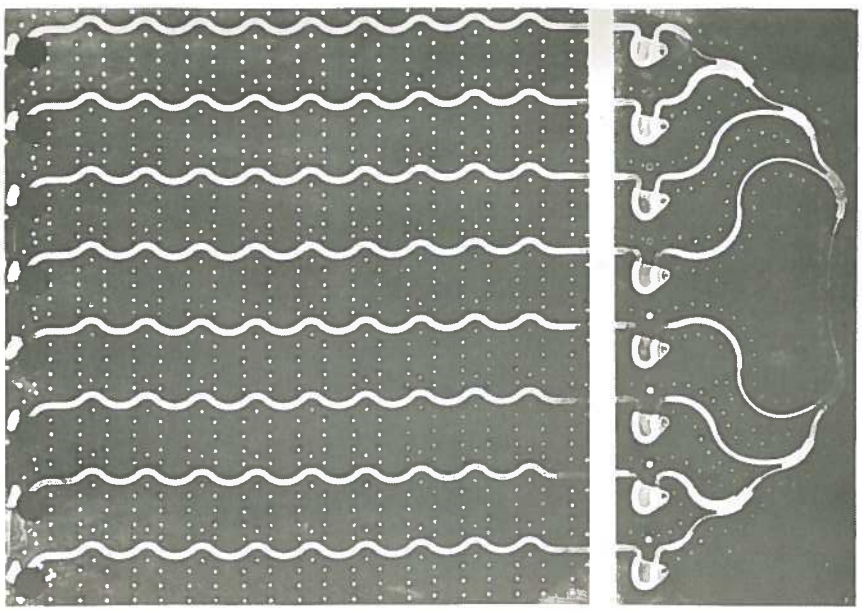

Figure 15 Disassembled 8 X 10 slot array (antenna A,B)

The correct value of k to be used for theoretical calculations is difficult to ascertain because the electrical location of the lumped series element in Fig. 1 is not precisely known. A serpentine structure, as shown in Fig. 15 for the 8 X 10 slot array, was used for the center strip, to produce a squint of $\sim 5^\circ$ with $d = 1.531$ inches in Rexolite 1422. The value of k used for the serpentine design was 1.10. Theoretical aperture distribution and radiation patterns were calculated for slot resistances used. These are shown in Figs. 13 and 14 for an optimum $k = 1.12$. Good agreement between theory and experiment is noted, indicating the adequacy of the mathematical model used in section 2. This one-dimensional array (see Fig. 12) used a long tapered strip of synthane as a sliding flat load.

Two-Dimensional 8 X 10 Slot Array

The two-dimensional array required only the additional design of a parallel feed structure and the utilization of a U bend, phase shifter, and flat load described earlier in section 3. Eight rows of slots with 2.06-inch spacing were used to fill the 17 X 17 inch aperture. The parallel feed structure was designed to give a -25 db S/L Tschebyscheff aperture distribution, and was connected using equal line lengths from the feed point for wideband H-plane performance. Power to individual rows and to portions of the feed (see Fig. 15), as well as corresponding characteristic admittances used for the strip transmission line, are given in Table IV.

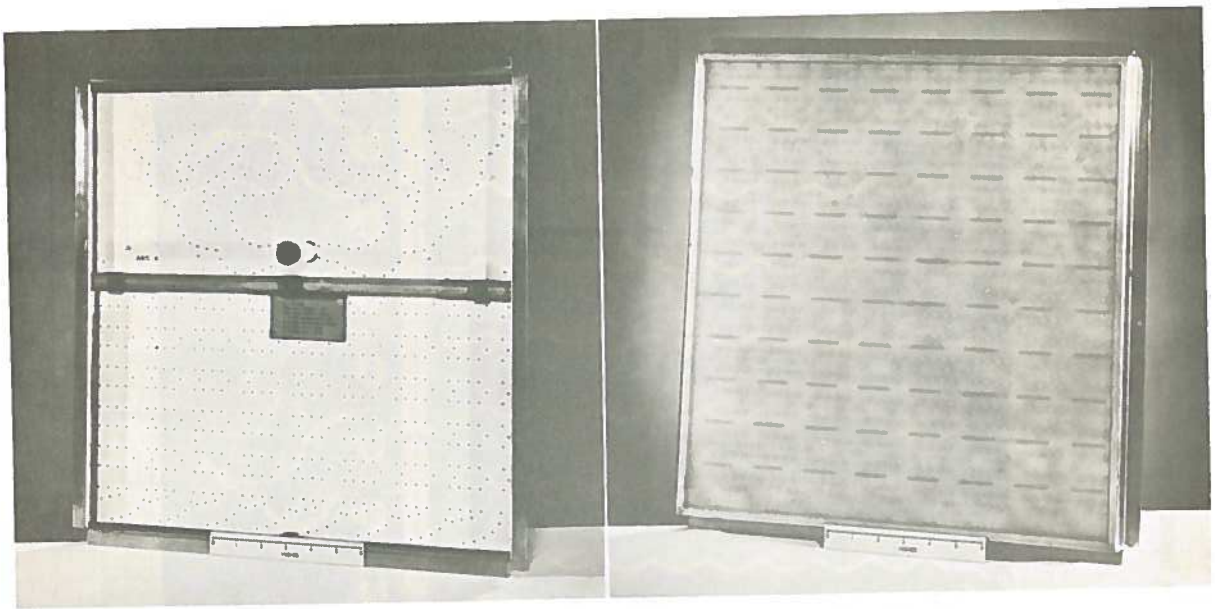

(a) Antennas A, B with U bend and phase shifters

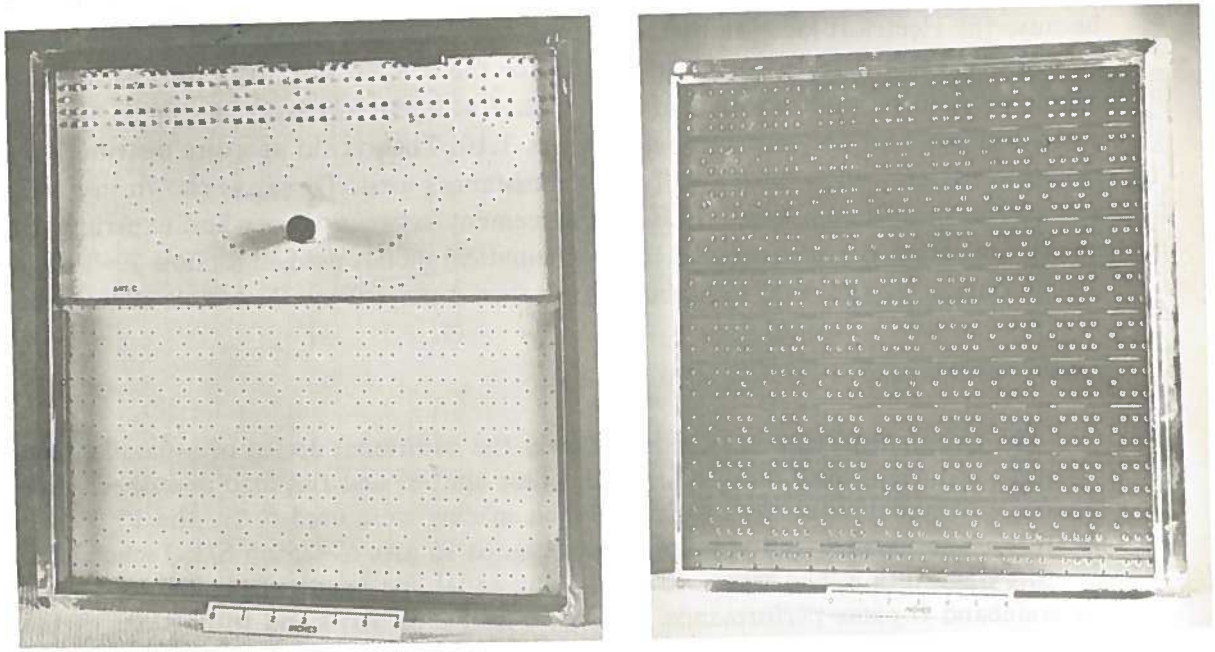

(b) Antenna C with slot coupling no phase shifters

Figure 16 Completed 8 X 10 slot array

TABLE IV

Power and admittance used in the 8-row parallel feed

Row No.	P	Y_0	P	Y_0	P	Y_0	P	Y_0	P	Y_0
1	.03254	.02/.011	.1103	.0373/.012						
2	.0778	.02/.0263			.272	.0296/.0167				
3	.1617	.02/.0176					.50	.0307/.01		
4	.2279	.02/.0140							1.0	.02
5	.2279	.02/.0140								
6	.1617	.02/.0176					.50	.0307/.01		
7	.0778	.02/.0263			.272	.0296/.0167				
8	.03254	.02/.011	.1103	.0373/.012						

The slashes in Table IV indicate 3-step binomial transformers [14], which are shown in the feed portion of Fig. 15. No compensation was made for step reactance in these transformers. The 360° phase shifters used can also be seen in Fig. 15. A poor H-plane aperture distribution was obtained until coupling between rows in the vicinity of the phase shifters was eliminated by the addition of eyelets. The distribution finally obtained is shown in Fig. 13b. The discrepancy between theoretical and measured cases is due to one or more of the following.

- small external and possibly internal coupling between slots.
- binomial transformers and Y junctions have lumped reactances at steps in strip width which were neglected.
- mismatch due to excess contact resistance in phase shifters.

The first models of the 8 X 10 slot array (Fig. 16, antenna A,B) employed a U bend and phase shifters so that phase shifts in the parallel feed could be compensated for. A third model of this array (antenna C) employed slot coupling between feed and radiating sections for each of the eight rows, and no phase shifters. This model was much easier to assemble and required no adjustment. E-plane patterns for antenna C showed a 3-db sidelobe improvement over antennas A and B, indicating better phasing between rows.

Stripline terminations employed in all these 8 X 10 slot arrays are those described in the latter part of section 3d. The average input VSWR from 4.15 to 4.25 GHz for these arrays is $\sim$1.6.

Mounting Configurations

Two of these 17 X 17 inch arrays are used for independent transmission and reception in low-altitude surveying. They are mounted close to each other in the H plane for minimum coupling. The isolation vs separation characteristic is given in Fig. 17.

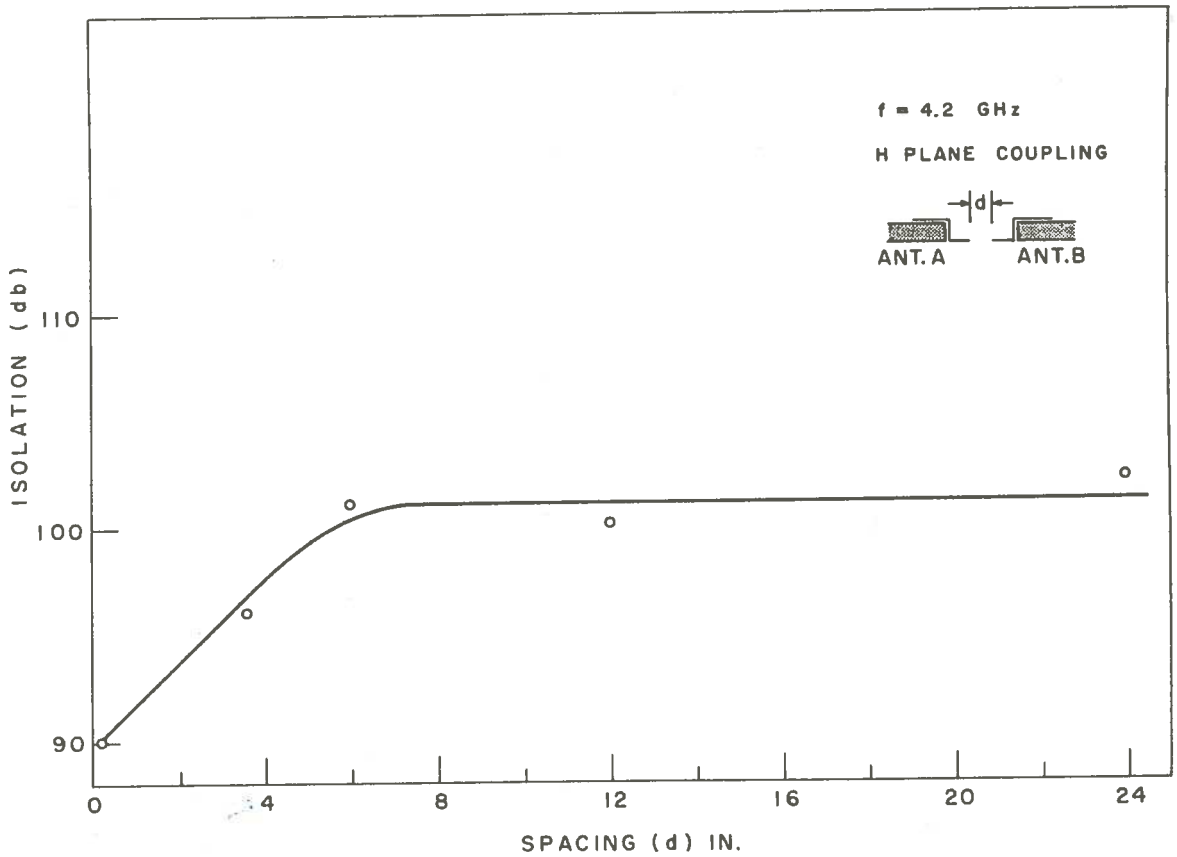

Figure 17 Isolation between two 8 X 10 slot arrays

The effect of using a thick Fiberglas sheet for aperture protection was observed by taking E-, H-plane patterns at 4.2 GHz. The results are given in Table V.

TABLE V

Sidelobe levels for a Fiberglas aperture cover on the 8 X 10 slot array

Antenna C $f = 4.2$ GHz

	No Fiberglas	$\frac{1}{16}$-inch Fiberglas	$\frac{1}{8}$-inch Fiberglas
E plane S/L (db)	-25	-19	-21.3
H plane S/L (db)	-18.5	-16.2	-17.3

It was suggested that perhaps four 8 X 10-slot antennas could be fed in phase in a four-element matrix to obtain characteristics somewhat similar to those described in section 5 for high-altitude surveying. This was tested by obtaining an interference pattern between antennas A and B fed in phase and adjacent to each other in the H plane. Three well defined beams appeared yielding only -5.5-db sidelobes, indicating that the present

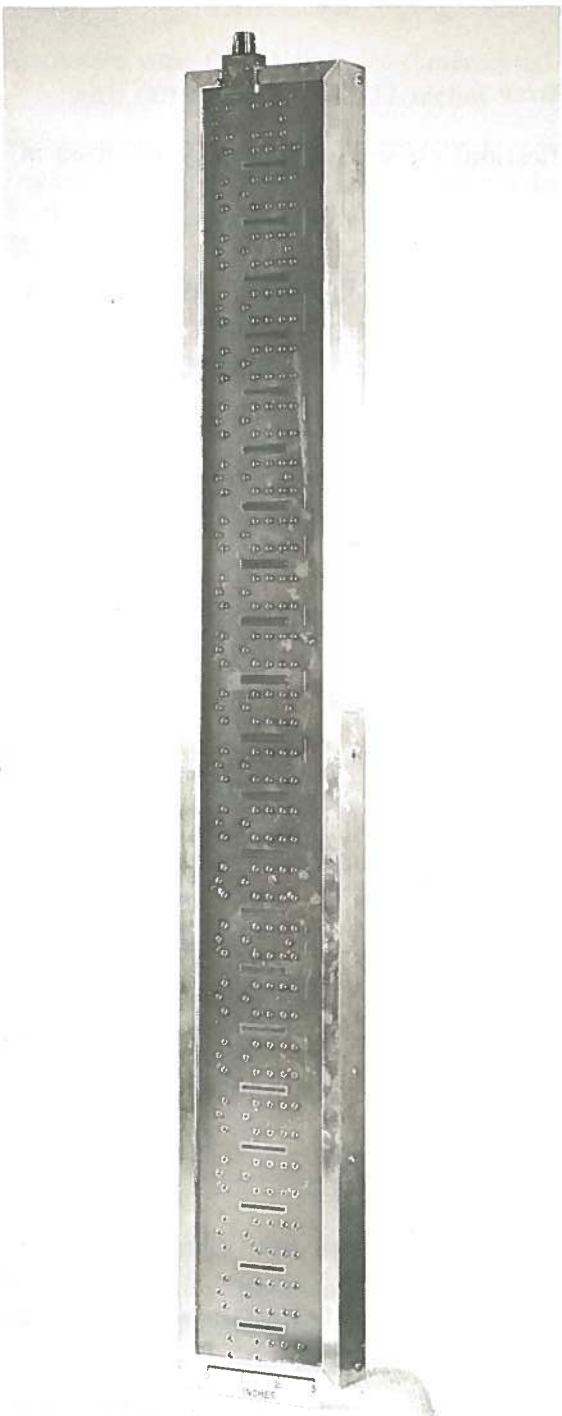

Figure 18 One-dimensional 21-slot array

symmetrically designed aperture distributions of antennas A, B, and C are not suitable for this purpose.

5. 16 X 21 Slot Array

General specifications chosen for this array are given in Table VI.

TABLE VI

General specifications of 16 X 21 slot array

f_0	4.2 GHz
Δf	5%
3 db beamwidth	$<5°$
P_{avg}	3 w
P_{peak}	5 kw
P_{load}	10%
θ_s	5°
aperture distribution	Taylor -18 db S/L
sidelobes desired	-14 db
slots/row	21
no. rows	16
d	1.531 inch
row spacing	2.060 inch
aperture size	34 X 34 inch
ϵ_r	2.53 (Rexolite 1422)
k	1.10 (nominal) = $\frac{\text{serpentine length}}{d}$
b	0.250 inch

One-Dimensional 21-Slot Array

The model containing the final slot data which were used in the 16 X 21 slot array will be described here, and is shown in Fig. 18.

Slot resistances for this 21-slot one-dimensional array were originally calculated assuming matched radiating elements, and then modified experimentally to produce an acceptable aperture distribution and radiation pattern. The -18-db S/L Taylor aperture distribution desired, for $\overline{n} = 5$ [15], plus slot resistances, slot offsets, and slot lengths used (see Fig. 5 and reference 10), are given in Table VII.

TABLE VII

Slot parameters used for 21-slot one-dimensional array with slot length $a' = 1.27$ inches

Slot No.	-18 db S/L Taylor aperture distribution desired (fld.)	Slot resistance used $\mathrm{Re}(Z_n)$	Slot reactance used $\mathrm{Im}(Z_n)$	Slot offset used d (inch)
1	0.982	0.0191	0.005	0.697
2	0.873	0.015	0.005	0.711
3	0.790	0.0122	0.005	0.720
4	0.796	0.0122	0.005	0.715
5	0.883	0.0158	0.005	0.705
6	0.996	0.0205	0.005	0.690
7	1.075	0.026	0.005	0.676
8	1.123	0.028	0.005	0.665
9	1.161	0.034	0.003	0.655
10	1.196	0.042	0	0.642
11	1.214	0.048	-0.003	0.636
12	1.196	0.052	-0.004	0.637
13	1.161	0.055	-0.005	0.637
14	1.123	0.058	-0.006	0.636
15	1.075	0.065	-0.007	0.633
16	0.996	0.070	-0.0075	0.626
17	0.883	0.075	-0.0075	0.622
18	0.796	0.083	-0.008	0.612
19	0.790	0.135	-0.008	0.592
20	0.873	0.235	-0.023	0.558
21	0.982	0.405	-0.053	0.530

In this case a constant slot length was used, so the elements were not quite resonant, as shown in Table VII. The experimental and theoretical E-plane aperture distributions and radiation patterns obtained for $f = 4.2$ GHz, $k = 1.12$ (optimum), and $\alpha = 0.033$ db/inch are shown in Figs. 19a and 20a. Note that the theoretical results were calculated for those values of Z_n actually used. The E-plane aperture distribution and radiation patterns are presented for the 16 X 21 slot array only, as the results for the one-dimensional 21-slot array were similar. Agreement between theory and experiment is seen to be good.

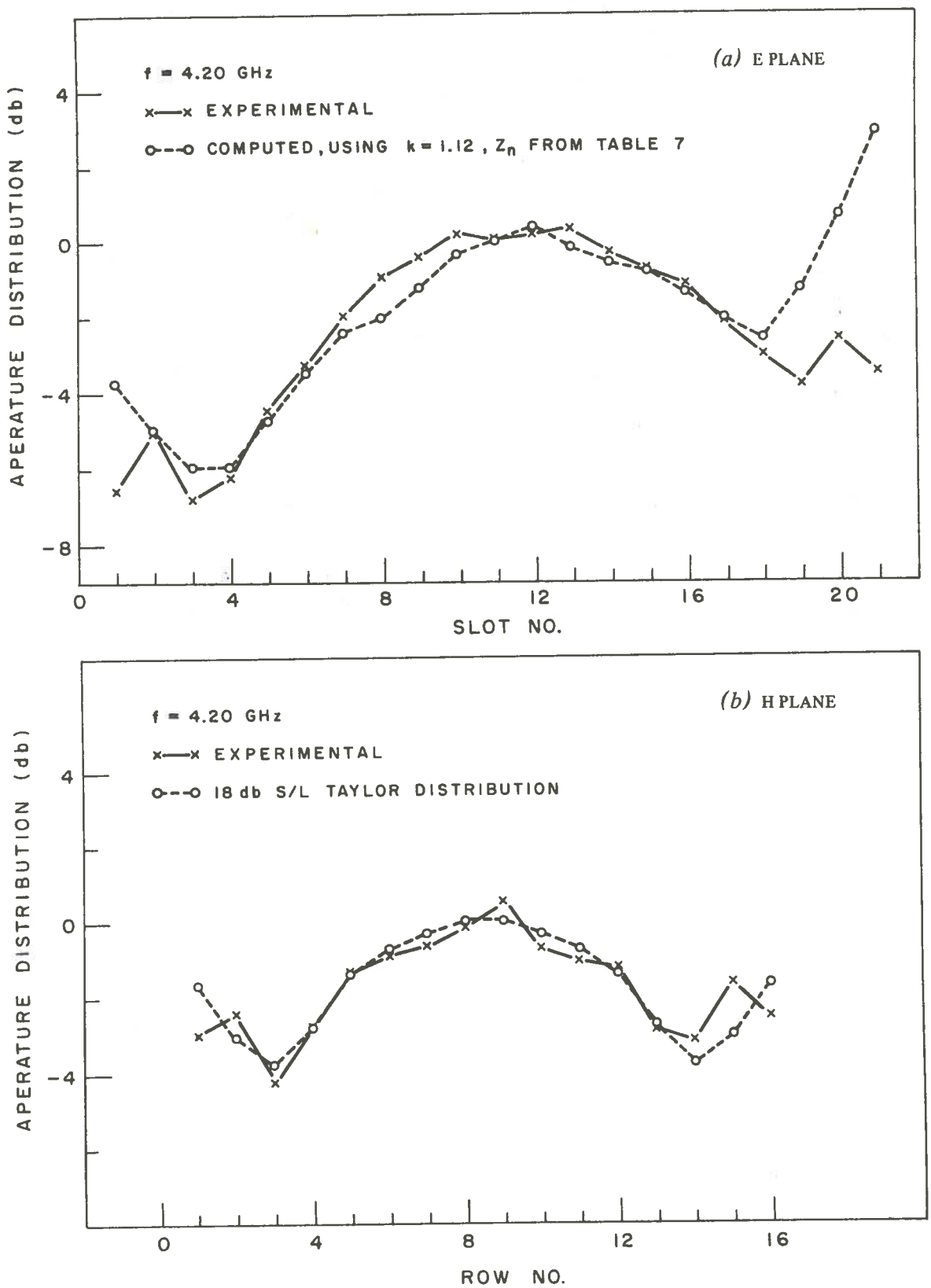

Figure 19 Aperture distributions of the 16 X 21 slot array

Two-Dimensional 16 X 21 Slot Array

The parallel feed section employed for this array contains no phase shifters, and resonant slot coupling to the radiating section. Sixteen rows spaced at 2.06 inches were excited using a -18-db S/L Taylor aperture distribution ($\bar{n} = 5$). Power and characteristic admittances used in various parts of this feed are given in TableVIII. For economy of space, the gradual bends of the 8 X 10 slot array's parallel feed were replaced by 90° mitered corners [16]. Slashes in Table VIII indicate positions where three-step binomial impedance transformers are inserted.

TABLE VIII

Power and admittances used in the 16-row parallel feed

Row No.	Y_0	P	Y_0	P	Y_0	P	Y_0	P	Y_0	P
1	.060	.02/.0161	.105	.0279/.0154						
2	.044	.02/.0118			.189	.0279/.0106				
3	.037	.02/.0123	.084	.0279/.0125						
4	.047	.02/.0156					.500	.0279/.01		
5	.064	.02/.0129	.139	.0279/.0125						
6	.075	.02/.0150			.311	.0279/.0173				
7	.082	.02/.0134	.171	.0279/.0154						
8	.089	.02/.0145							1.00	.02
9	.089	.02/.0145	.171	.0279/.0154						
10	.082	.02/.0134			.311	.0279/.0173				
11	.075	.02/.0150	.139	.0279/.0125						
12	.064	.02/.0129					.500	.0279/.01		
13	.047	.02/.0156	.084	.0279/.0125						
14	.037	.02/.0123			.189	.0279/.0106				
15	.044	.02/.0118	.105	.0279/.0154						
16	.060	.02/.0161								

Steps in transmission line width and mitered corners did not cause enough amplitude or differential phase error to affect seriously the H-plane aperture distribution or radiation patterns, as seen in Figs. 19b and 20b, respectively. The stripline terminations used were described earlier in the latter part of section 3d.

Input VSWR to this array (unmatched) is 1.15 at 4.2 GHz, and is ∿1.45 average from 4–4.5 GHz.

When a $\frac{1}{16}$-inch Fiberglas cover is added for aperture protection, input VSWR decreases, and E-plane sidelobes rise from -15.5 to -12 db at 4.2 GHz. This completed array, with a thin Mylar aperture cover, is shown in Fig. 21.

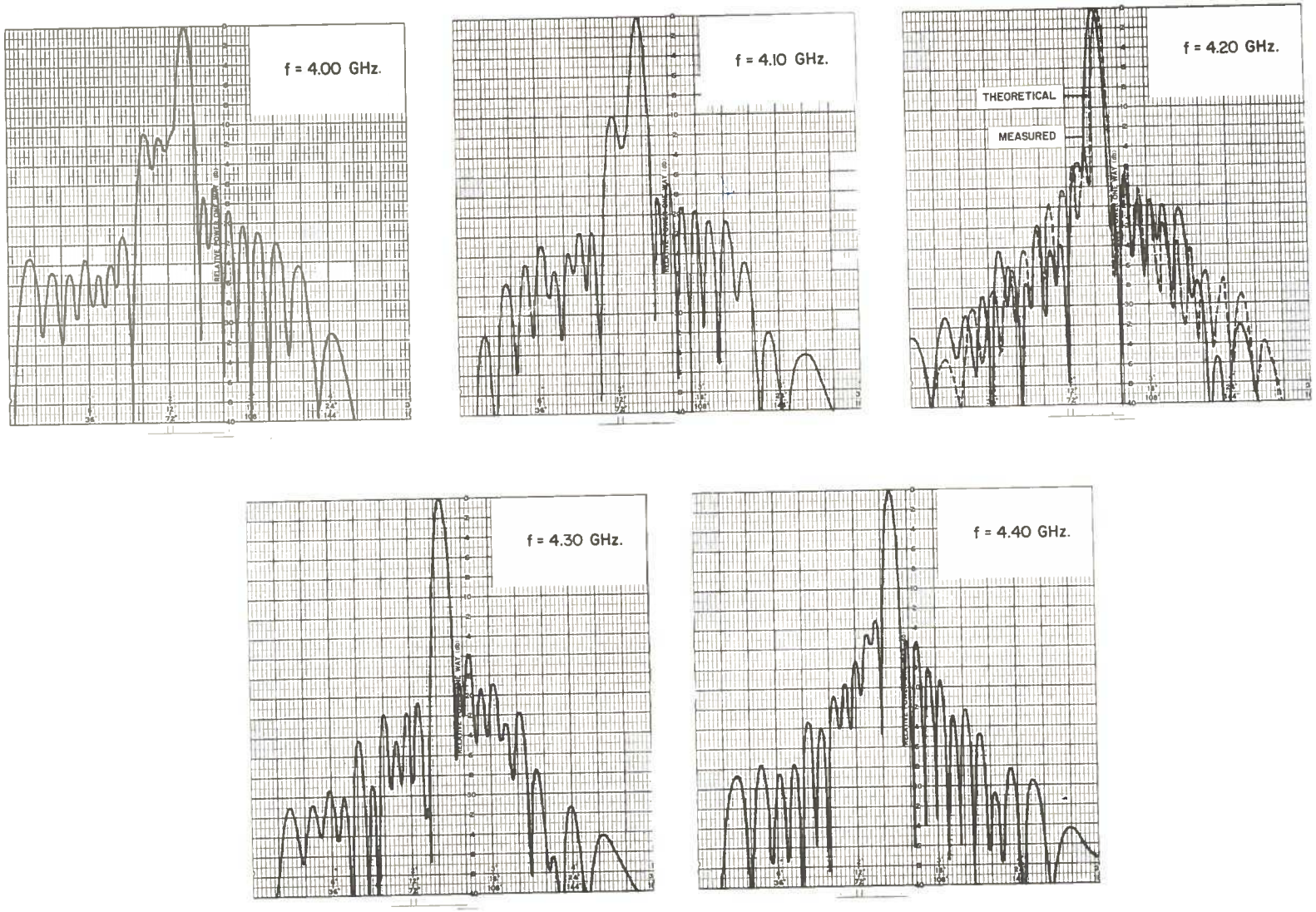

Figure 20 (a) Radiation patterns of the 16 X 21 slot array, E plane

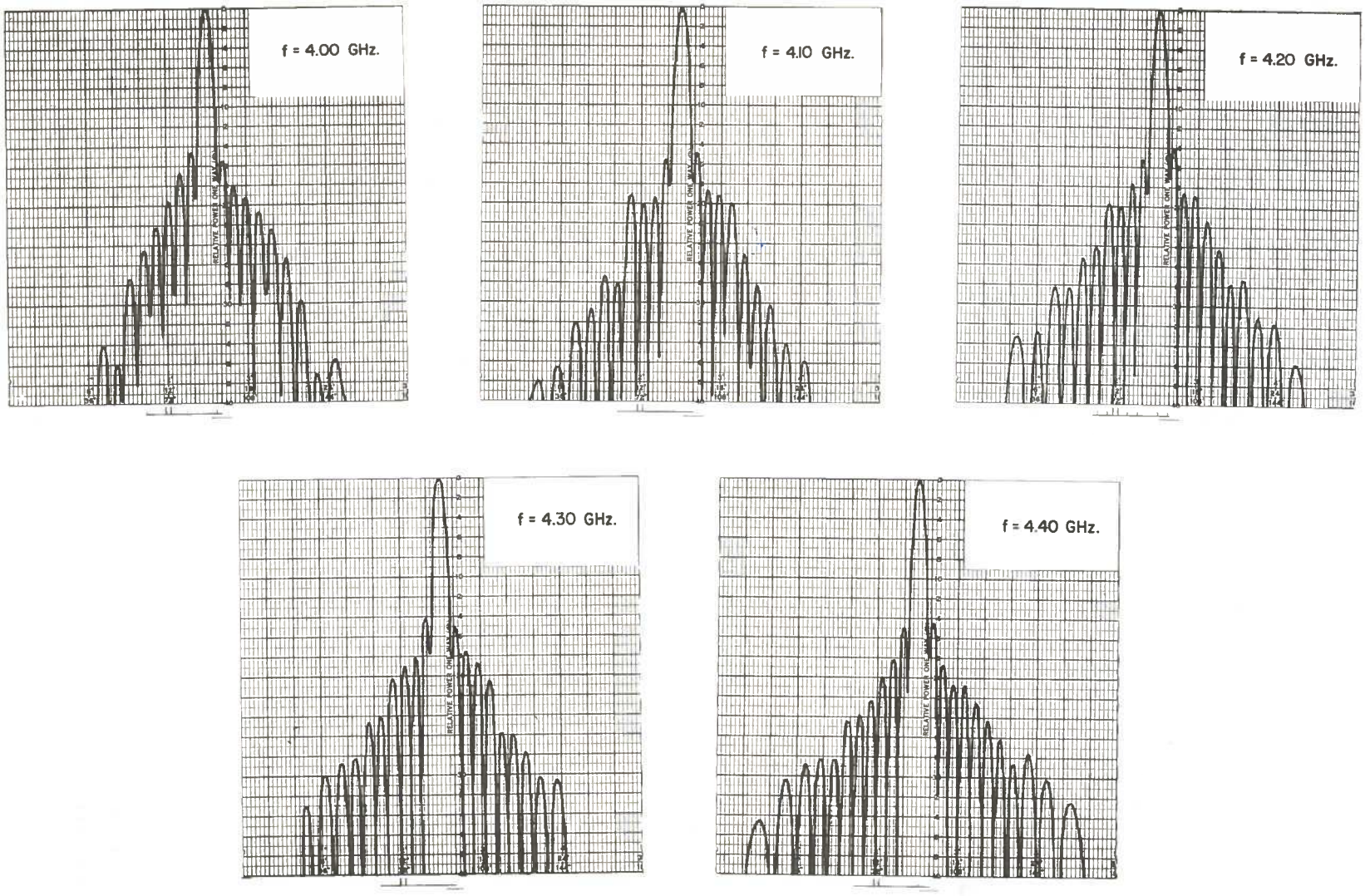

Figure 20 (b) Radiation patterns of the 16 X 21 slot array, H plane

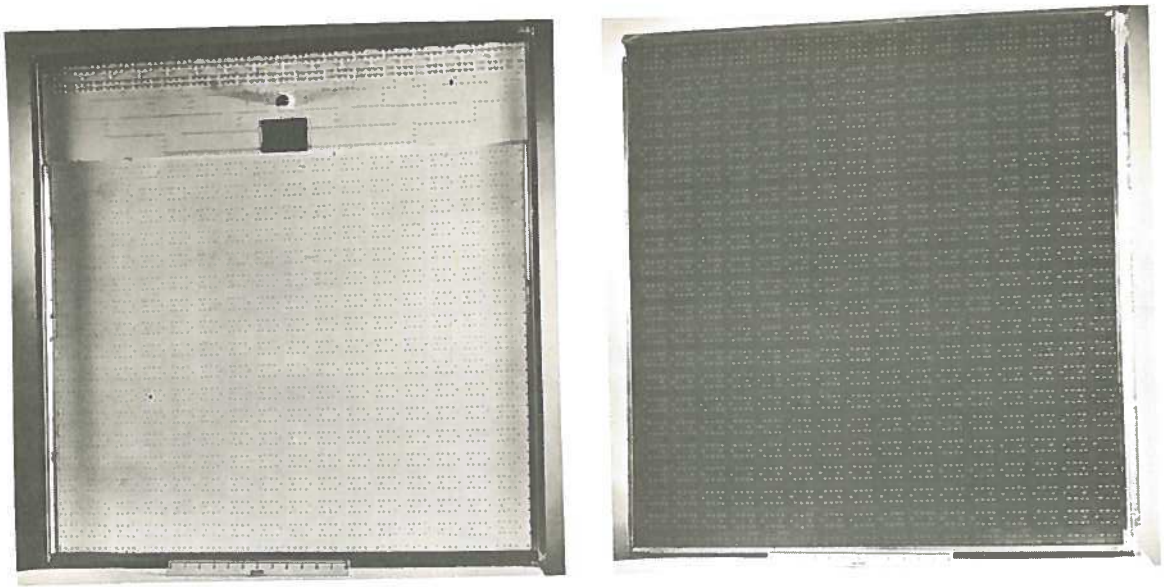

Figure 21 Completed 16 X 21 slot array

Acknowledgment

The authors are indebted to G.C. McCormick for suggesting much of the array analysis and for many discussions of this work.

References

1. Westby, R.L. A radar altimeter for forest inventory. Bulletin of the Radio and Electrical Engineering Division, National Research Council, 17 (1): 46–49; 1967.
2. Westby, R.L. Radar altimeter. Bulletin of the Radio and Electrical Engineering Division, National Research Council, 17 (3): 70–71; 1967.
3. Westby, R.L. Test results of radar altimeter for forest inventory in tropical rain forests. Bulletin of the Radio and Electrical Engineering Division, National Research Council, 18 (2): 1–2; 1968.
4. Sanders Associates Inc., Handbook of Triplate Microwave Components, 1956.
5. Harvey, A.F. Microwave engineering. Academic Press, 1963.
6. Jones, H.S. Integrated radome antenna design. Microwaves, 6 (9): 34–39; 1967.
7. Johnson, H.P. An extremely thin flush mounted slotted linear array. Abstracts of the Sixteenth Annual Conference on Antenna Research and Development, 1966.
8. Breithaupt, R.W. and Clarke B. A two dimensional stripline altimeter antenna. Bulletin of the Radio and Electrical Engineering Division, National Research Council, 18 (2): 9–16; 1968.
9. McCormick, G.C. and Breithaupt, R.W. Traveling wave arrays of mismatched elements (to be published).

10. Breithaupt, R.W. Conductance data for offset series slots in stripline. IEEE Trans. MTT-16 (11): 969–970; 1968.
11. Craven, J.H. Stripline provides microwave components quickly and easily. Electron. and Commun., 8: 44–53; 1960.
12. Altschuler, H.M. and Oliner, A.A. Discontinuities in the centre conductor of symmetric strip transmission line. Polytechnic Institute of Brooklyn, Microwave Research Institute, Research Report R-749-59: PIb-677; 1959.
13. Brown, L.B. and Scharp, G.A. Tschebyscheff antenna distribution, beamwidth, and gain tables. NAVORD Rept. 4629, 28 February 1958.
14. Young, L. Practical design of a wideband quarter-wave transformer in waveguide. Microwave J., 6: 76–79; 1963.
15. Spellmire, R.J. Tables of Taylor aperture distribution. Hughes Aircraft Co., T.M. No. 581, October 1958.
16. Keen, H.S. Scientific report on study of strip transmission lines. Cambridge Air Force Research Center, AF 19 (604)-780 Report No. 2830 –2, December 1, 1955.

PROGRAMME FOR 21 SLOT ARRAY

```
C *** CALC FOR APERT. DIST ASSUMING  MISMATCH AT ELEMENTS
C *** BLAM - GUIDE WAVELENGTH
C *** SEN - POWER TO THE LOAD
C *** DIN(I) - ELECTRICAL SPACING BETWEEN SLOTS
C *** RED(I) - CALC. SLOT RESISTANCE ASSUMING  NO REFLECTIONS
C *** SIA - TRANS. AMPL. ON RHS OF SLOT MODULE
C *** SIB - REFL AMPL. ON RHS OF SLOT MODULE
C *** SIAT AND SIBT  - AS ABOVE BUT FOR LHS OF SLOT MODULE
C *** VSWR - VSWR INTO LHS OF SLOT MODULE
C *** FET - AMPL. OF RAD. FIELD FROM SLOT
C *** FETA(I) -  PHASE OF RAD. FIELD FROM SLOT
C *** FETM - ABS. VALUES OF RAD. FIELD FROM SLOTS
C *** ATT= EXPONENT GIVING FLD. ATTEN BETWEEN SLOTS
C *** THETA= ELECT ANGLE BETWEEN SLOTS IN RADIANS
C *** ATTT(I)   VARIABLE VALUES OF ATT TO BE USED IF DESIRED
C *** CONST(KTK) IS THE EFFECTIVE SHORTENING OF LAMBDA G DUE TO
C      THE SERPENTINE STRUCTURE BETWEEN ELEMENTS


      DIMENSION TEXT(30),TEXT1(30),TEXT2(30),TEXT3(30),XPAR(10),YPAR(10)
     1,TEXT5(30),BUF(80),DB(180),ANGL(180)
      COMPLEX SIBT
      COMPLEX ZED(26),TEL(26),TEN(26),SIA,SIB,FET,SIAT,SIAB,CRRED(26),
     1CEN(26),ETHEL(180),EX,FII
C *** FETO(I) IS THE DESIRED FIELD APERTURE DISTRIBUTION
      REAL FETO(21)/.982,.873,.790,.796,.883,.996,1.075,1.123,1.161,
     $1.196,1.214,1.196,1.161,1.123,1.075,.996,.883,.796,.790,.873,.982/
C *** XED(I) IS THE  SLOT REACTANCE TO BE USED
     1,XED(21)/.005,.005,.005,.005,.005,.005,.005,.005,.003,0.0,
     1-.003,-.004,-.005,-.006,-.007,-.0075,-.0075,-.008,-.008,-.023,
     1-.053/
      REAL  DIN(21),RED(21),FETA(21)
C *** RRN(21) ARE VALUES OF SLOT RESISTANCE TO BE INSERTED IF AN APERTURE
C      DIST. AND RAD. PATTERN IS DESIRED FOR THEM - SEE PART 2
      REAL RRN(21)
     1       /.0191,.015,.0122,.0122,.0158,.0205,.026,.028,.034,
     1.042,.048,.052,.055,.058,.065,.070,.075,.083,.135,.235,.405/
      REAL ATTL(21)
      REAL CONST(10)


C *** PART 1  SLOT RESISTANCES RRED, SRED, CALCULATED TO GIVE FLD AMP
C      FETO(I) FOR GIVEN VALUES OF DIN(I),XED(I)
      DO 307 KTK=1,5
      CONST(KTK)=1.1+.01*KTK
      BLAM=1.767/CONST(KTK)
      SEN=2.373
      FREQ=4.2
      SIA=(1.540,0.0)
      SIB=(0.0,0.0)
C      FOR REXOLITE 1422 ATT=.00633 THEORETICAL
      ATT=.00633*CONST(KTK)
  205 FORMAT(' SLOT FLD ASK   R NO REF    REACT   FLD GOT     PHASE   V
     1SWR     R CALC 1  R CALC2  DIN(I)   INDEX')
      WRITE(3,205)
      DO 40 II=1,21
      I=22-II
      DIN(I)=1.531
      DIST=1.531
      DIN(I)=DIST
      PI=3.14159263
      RRED=FETO(I)*FETO(I)/(CABS(SIA-SIB))**2
      CRRED(I)=RRED
      ZED(I)=CMPLX(RRED,XED(I))
  203 CONTINUE
      ATT=.00633*DIN(I)/DIST
      THETA=6.28319/BLAM*DIN(I)
      TEL(I)=CEXP(CMPLX(ATT,THETA))
      TEN(I)=CEXP(CMPLX(-ATT,-THETA))
      SIAT=((1.0+ZED(I)/2.)*SIA-ZED(I)/2.*SIB)*TEL(I)
      SIBT=(ZED(I)/2.*SIA+(1.-ZED(I)/2.)*SIB)*TEN(I)
      ATTL(I)=(CABS(SIAT))**2*(1-EXP(-2*ATT))-(CABS(SIBT))**2*( 1-EXP
     $(2*ATT))
      RED(I) =FETO(I)*FETO(I)/SEN
      SEN=SEN+FETO(I)*FETO(I)+ATTL(I)
      SRED=RED(I)*(((CABS(SIA))**2-(CABS(SIB))**2)/(CABS(SIA-SIB))**2)
      FET=(SIA-SIB)*SQRT(RRED)
      FETA(I)=ATAN2(AIMAG(FET),REAL(FET))*180./3.14159
      FETM=CABS(FET)
      SIA=SIAT
      SIB=SIBT
      VSWR=CABS(SIB)/CABS(SIA)
      VSWR=(1.0+VSWR)/(1.0-VSWR)
      WRITE(3,7) I,FETO(I),RED(I),XED(II),FETM,FETA(I),VSWR,RRED,SRED,
     $DIN(I),INDEX
    7 FORMAT(I5,9F10.4,I5)
   40 CONTINUE
      WRITE(3,302)
  302 FORMAT('  PHYSICAL SPACING= 1.531')


C *** PART 2
C *** CALCULATE APERTURE DIST AND E FIELD RAD. PATTERN OF ARRAY
C      - OR THIS SECTION CAN BE USED TO CALC APERT. DIST AND RAD. PATTERN
C      FOR AN ARB. SET OF SLOT RESIST. RRN(I) AND REACT. XED(I).
C      INSERT 'ATT=ATTT(I)' AFTER  'I = 22-J' IF DESIRED
      JJ=1
C****BLAMF=FREE SPACE WAVELENGTH
      BLAMF=BLAM*SQRT(2.53)*CONST(KTK)
      THETAP=6.283186/BLAM*DIN(I)
      SIA=(1.540,0.0)
      SIB=(0.0,0.0)
      DO 14 J=1,21
      I=22-J
      CRRED(I)=RRN(I)
      ATT=.00633*DIN(I)/DIST
      ZED(I)=CMPLX(RRN(I),XED(I))
      TEL(I)=CEXP(CMPLX(ATT,THETAP))
      TEN(I)=CEXP(CMPLX(-ATT,-THETAP))
```

```
      CEN(I)=(SIA-SIB)*CSQRT(CRRED(I))
      SIAT=((1.+ZED(I)/2.)*SIA-ZED(I)/2.*SIB)*TEL(I)
      SIBT=(ZED(I)/2.*SIA+(1.-ZED(I)/2.)*SIB)*TEN(I)
      SIA=SIAT
      SIB=SIBT
   14 CONTINUE
      VSWR=(1.0+CABS(SIB/SIA))/(1.0-CABS(SIB/SIA))
      XEX=(6.283185-THETAP)/6.283185*29.98/(FREQ*2.54)
      FI=ARCOS(XEX/1.531)
      FII=(0.0,0.0)
  308 FORMAT(///' APERTURE DISTRIBUTION IN DB FOR F(GHZ)= ',F3.1/)
      WRITE(3,308)FREQ
  309 FORMAT(' SLOT NO.       POWER(DB)      SLOT RESIST     SLOT REACT'/)
      WRITE(3,309)
      DO 19 MM=1,21
      YEY=10*ALOG10((CABS(CEN(MM)))**2/(CABS(CEN(11)))**2)
  310 FORMAT(3X,I3,11X,F6.3,10X,F6.3,10X,F6.3)
      WRITE(3,310) MM,YEY,PRN(MM),XED(MM)
      EX=CEN(MM)*CEXP(CMPLX(0.0,-(MM-11)*1.531*6.283185/BLAMF
     1*COS(FI)))
   19 FII=FII+EX
      FII=(SIN(FI)+.0000001)*FII
      DO 16 M=1,179
      THETA=(M-1)/57.29578
      ITA=M-1
      ETHEL(M)=(0.0,0.0)
      DO 17 MM=1,21
      EX=CEN(MM)*CEXP(CMPLX(0.0,-(MM-11)*1.531*6.283185/BLAMF
     1*COS(THETA)))
   17 ETHEL(M)=ETHEL(M)+EX
      ETHEL(M)=(SIN(THETA)+.0000001)*ETHEL(M)
      PHETA=20.*ALOG10(CABS(ETHEL(M)/FII))
      DB(M)=-PHETA
      ANGL(M)=ITA
   18 FORMAT(//8X,I3,3F12.4)
   16 CONTINUE
  301 FORMAT('  F=      GHZ',F3.1)
  303 FORMAT('  ELECTRICAL SPACING=        ',F6.4)
  304 FORMAT('  INPUT VSWR=        ',F8.4)
C *** ARRANGED TO GIVE SIX PLOTS IF DESIRED
      GO TO (110,111,112,113,114,115),JJ
  110 XPAR(1)=1.0
      YPAR(1)=1.0
      GO TO 116
  111 XPAR(1)=11.0
      YPAR(1)=1.0
      GO TO 116
  112 XPAR(1)=21.0
      YPAR(1)=1.0
      GO TO 116
  113 XPAR(1)=1.0
      YPAR(1)=12.0
      GO TO 116
  114 XPAR(1)=11.0
      YPAR(1)=12.0
      GO TO 116
  115 XPAR(1)=21.0
      YPAR(1)=12.0
  116 XPAR(2)=7.0
      YPAR(2)=9.0
      XPAR(7)=.30
      YPAR(7)=.50
      XPAR(8)=8.0
      CALL GRID2(3,13.0,XPAR,YPAR)
      XPAR(3)=0.0
      YPAR(3)=0.0
      XPAR(4)=6.6667
      YPAR(4)=20.0
      XPAR(5)=3.0
      YPAR(5)=9.0
      CALL LINE2(DB,ANGL,180,XPAR,YPAR)
      XCOR=XPAR(1)
      YCOR=YPAR(1)-1.0
      CALL PSTART(XCOR,YCOR,8.,10.,XPAR(3),YPAR(3),XPAR(4),YPAR(4),IER)
      CALL INCORE(BUF,80)
      WRITE(3,105)
  105 FORMAT('M.M.STEEN RM 378 M50')
      CALL NAME2(BUF,30)
      CALL INCORE(BUF,80)
      WRITE(3,106)
  106 FORMAT(' THETA (DEGREES)')
      CALL PTEXT2(BUF,18,7.75,4.0,0.0,.15,2)
      CALL INCORE(BUF,80)
      WRITE(3,107)
  107 FORMAT('POWER INTENSITY (DB)')
      CALL PTEXT2(BUF,22,2.5,.25,.15,0.0,1)
      CALL INCORE(BUF,80)
      WRITE(3,108)
  108 FORMAT('0          -10          -20          -30          -40')
      CALL PTEXT2(BUF,50,0.0,.75,.125,0.0,1)
      CALL INCORE(BUF,80)
      WRITE(3,109)
  109 FORMAT('0       20       40       60       80       100      120      14
     10      160      180')
      CALL PTEXT2(BUF,78,7.25,1.0,0.0,.1233,2)
      CALL INCORE(BUF,80)
      WRITE(3,117)
  117 FORMAT(16H21 ELEMENT ARRAY)
      CALL PTEXT2(BUF,16,0.8,6.5,0.0,.15,2)
      CALL INCORE(BUF,80)
      WRITE(3,101)FREQ
  101 FORMAT(4HF = ,F3.1,4H GHZ)
      CALL PTEXT2(BUF,12,1.1,6.5,0.0,.15,2)
      CALL INCORE(BUF,80)
      WRITE(3,102)
  102 FORMAT(23HPHYSICAL SPACING= 1.531)
      CALL PTEXT2(BUF,23,1.4,6.5,0.0,.15,2)
      CALL INCORE(BUF,80)
      WRITE(3,103)DIN(I)
  103 FORMAT(21HELECTRICAL SPACING = ,F6.4)
```

```
      CALL PTEXT2(BUF,27,1.7,6.5,0.0,.15,2)
      CALL INCORE(BUF,80)
      WRITE(3,104)VSWR
  104 FORMAT(14HINPUT VSWR =   ,F8.4)
      CALL PTEXT2(BUF,22,2.0,6.5,0.0,.15,2)
      CALL PAGE
  307 CONTINUE
      CALL PEND
   12 CALL EXIT
      END
```